BNL-NUREG -32047
INFORMAL REPORT
Limited Distribution

CONTAINER ASSESSMENT - CORROSION STUDY OF HLW CONTAINER MATERIALS

QUARTERLY PROGRESS REPORT
JULY-SEPTEMBER 1982

T. M. AHN, B. S. LEE, AND P. SOO

NUCLEAR WASTE MANAGEMENT DIVISION

DEPARTMENT OF NUCLEAR ENERGY BROOKHAVEN NATIONAL LABORATORY
UPTON, NEW YORK 11973

Prepared for the U.S. Nuclear Regulatory Commission
Office of Nuclear Regulatory Research
Contract No. DE-AC02-76CH00016

NOTICE

Available from
GPO Sales Program
Division of Technical Information and Document Control
U.S. Nuclear Regulatory Commission
Washington, D.C. 20555
and
National Technical Information Service
Springfield, Virginia 22161

BNL-NUREG-32047
INFORMAL REPORT
Limited Distribution

CONTAINER ASSESSMENT - CORROSION STUDY OF HLW CONTAINER MATERIALS

QUARTERLY PROGRESS REPORT
July-September 1982

T. M. Ahn, B. S. Lee, and P. Soo

Manuscript Completed October 1982

Prepared by
The Nuclear Waste Management Division
D. G. Schweitzer, Head
Department of Nuclear Energy
Brookhaven National Laboratory
Associated Universities, Inc.
Upton, NY 11973

Prepared for the U.S. Nuclear Regulatory Commission
Office of Nuclear Regulatory Research
Contract No. DE-AC02-76CH00016
FIN No. A-3237

ABSTRACT

Crevice corrosion specimens consisting of Ti-Teflon and Ti-Ti couples have been exposed to simulated Waste Isolation Pilot Project (WIPP) Brine A at 150°C. Studies were conducted on the morphology and chemical identification of corrosion products formed within the crevice region. In the case of Ti-Teflon samples, anodic dissolution was observed and this is apparently followed by a hydrolysis reaction. The reaction results in the formation of rutile crystals and hydride precipitation beneath the oxide scale. For Ti-Ti crevice samples, there is mechanical failure of the anatase oxide due to the formation of blisters by hydrogen gas pressurization. The blisters fracture when the hydrogen pressure is sufficiently high and rutile is observed to precipitate on the crack surfaces. Based on these observations, a mechanism for Ti-Ti crevice corrosion is proposed. This involves macroscopic concentration cell formation accompanied by pH and electrode potential drops in the crevice region. Rutile scale becomes dominant and hydrides form beneath the scale.

The load-displacement curves for TiCode-12 single-edged-notched (SEN) samples with various hydrogen levels were analyzed. Based on fractographic analysis it was found that TiCode-12 is susceptible to hydrogen embrittlement above a hydrogen concentration level of about 200 ppm. Hydride formation is considered to be responsible for the embrittlement observed.

The effects of contamination on gamma-radiation-induced gas generation in WIPP Brine A has been discussed. Some preliminary data on solution chemistry changes upon gamma irradiation are presented.

CONTENTS

FIGURES

ACKNOWLEDGMENT

The authors gratefully acknowledge the assistance of G. Spira and R. Jones in the technical parts of the program and S. M. Moore for her skills in preparing the manuscript.

1. CREVICE CORROSION OF COMMERCIALLY PURE (CP) TITANIUM

In this quarter, most of the morphological studies on titanium crevice corrosion products and their identification have been completed. Based on these results, crevice corrosion mechanisms have been proposed for this metal during exposures to simulated Waste Isolation Pilot Project (WIPP) brine.

1.1 Ti-Teflon Crevices

Earlier work by Bohlman and Posey[1] shows that crevice corrosion of Ti-Teflon crevices in brine is more severe than that for Ti-Ti crevices. They also show that the increased rate of attack is likely to be a result of small amounts of fluoride released from the Teflon. In the present study, a similar effort was initiated for Ti-Teflon crevices exposed to WIPP Brine A at 150°C. Such a study is an important step in determining the crevice corrosion process in TiCode-12 high level waste container material.

Results to date confirm that Ti-Teflon crevices indeed show faster rates of crevice attack when compared to Ti-Ti couples. Typically, the Ti-Teflon samples display a ring of corroded metal (anodic dissolution) at the center of the crevice. This is surrounded by an adjacent area consisting of aggregates of small crystals approximately 2000-3000 Å in diameter. Figure 1 shows these aggregates which were examined by electron diffraction techniques in the transmission electron microscope and found to be the rutile form of TiO_2. From the morphology of the aggregates it appears that they were formed by precipitation from the brine solution. Adjacent to the rutile crystals, in regions closer to the perimeter of the crevice, large anatase TiO_2 crystals (1-3 μm in diameter) were identified by electron diffraction. In some areas, needle-shaped rutile was present above the anatase layer, as shown in Figure 2.

Based on these observations, and the electrochemical studies of other workers,[2,3] it is postulated that anatase crystals initially grow inside the crevice causing oxygen depletion, and eventually lead to the formation of a macroscopic concentration cell. As the oxygen depletion process proceeds, the pH and electrode potential decrease. When the potential at the center of the crevice becomes low enough, the anatase dissolves releasing a high concentration of titanium ions. This creates an electrode potential gradient with a lower potential at the center of the crevice. To preserve the electroneutrality condition, titanium ions migrate outward, and Cl^- ions migrate into the crevice from the bulk brine solution. A hydrolysis reaction follows and the rutile form of TiO_2 is precipitated in the form of small crystals (Figure 1). This is accompanied by the production of HCl. The stability of rutile at the low potential condition is in accord with other work which shows that rutile is more stable than anatase at lower potentials.[4] Because of the hydrolysis reaction, the pH of the solution near the rutile particles decreases (probably to a value as low as 1) and the anatase adjacent to the rutile begins to transform to rutile also. This rutile continues to form and a needle-like morphology is produced as shown in Figure 2. Since the electrode potential inside the crevice is so low the H^+ reduction reaction

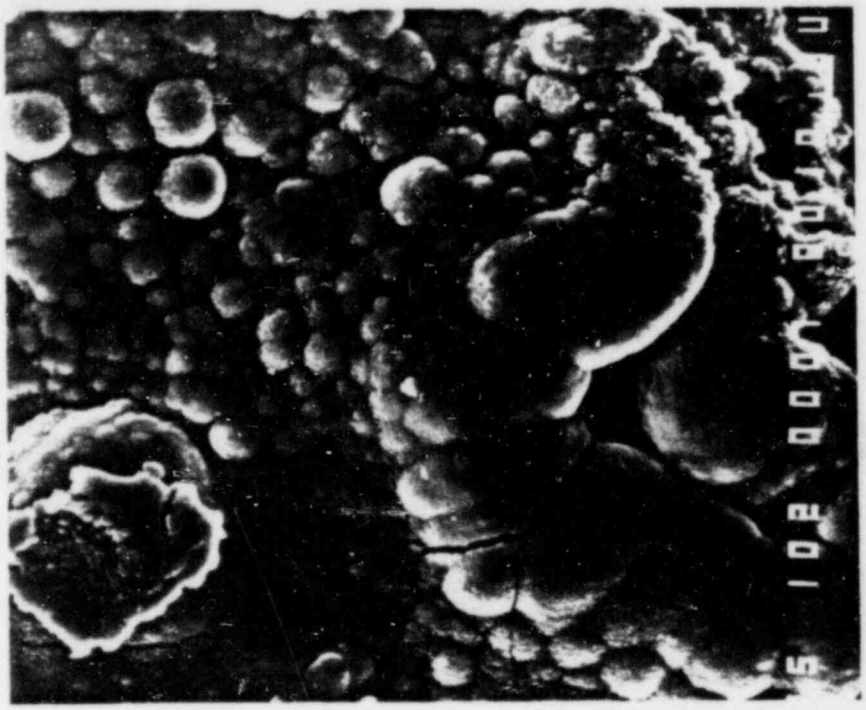

Figure 1. Aggregates of very small rutile crystals formed in Ti-Teflon crevices during adjacent anodic dissolution in crevices exposed to WIPP Brine A at 150°C. Magnification 1000 X.

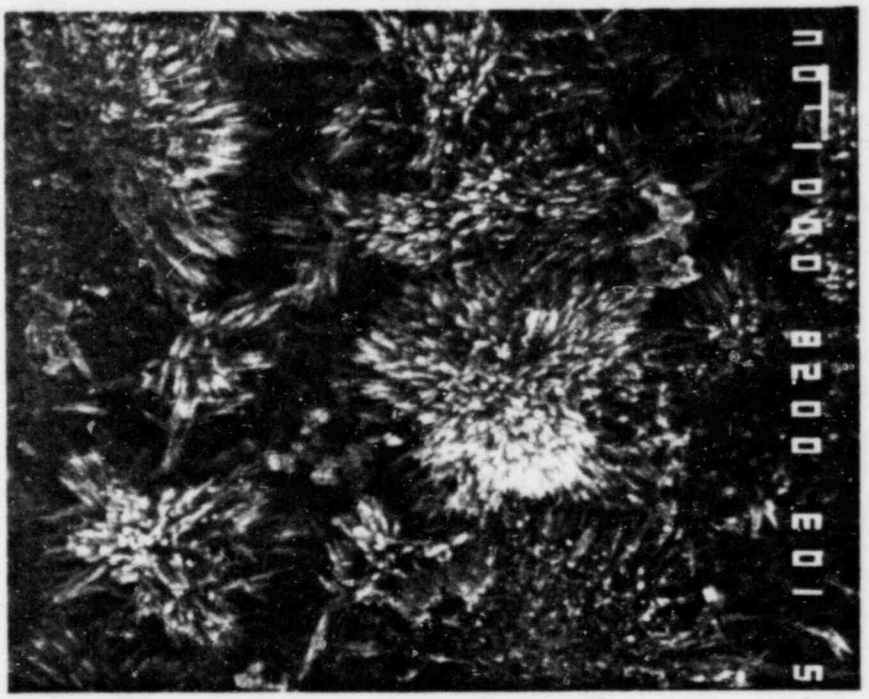

Figure 2. Needle-shaped rutile crystals formed on the anatase layer in Ti-Teflon crevices exposed to WIPP Brine A at 150°C. Magnification 10000 X.

becomes cathodic and generates H_2 gas and atomic H. The latter is thought to be responsible for hydride formation beneath the oxide scale as shown in Figure 3. The hydride probably causes the catastrophic disintegration of the titanium which is observed after removal of samples from the solution. Bohlman and Posey also observed hydride formation beneath oxide scales in their work.[1]

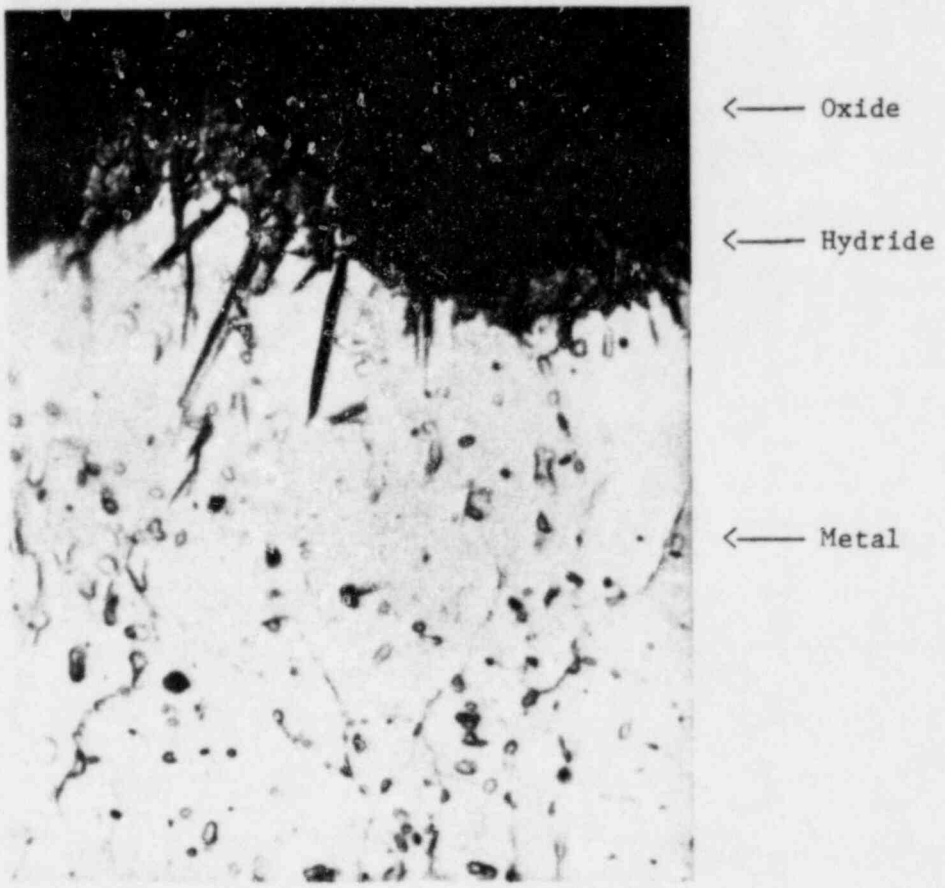

Figure 3. Cross section of a severely attacked Ti-Teflon crevice sample after exposure to WIPP Brine A for four weeks at 150° . Needle-shaped crystals are thought to be hydrides. Magnification 100 X.

1.2 Ti-Ti Crevices

The morphology of Ti-Ti crevice corrosion products formed after severe attack is quite different from that observed for Ti-Teflon specimens. No oxide or metal dissolution was observed. Instead, the anatase scale contains blisters which eventually crack (Figure 4). Figure 5 shows a magnified

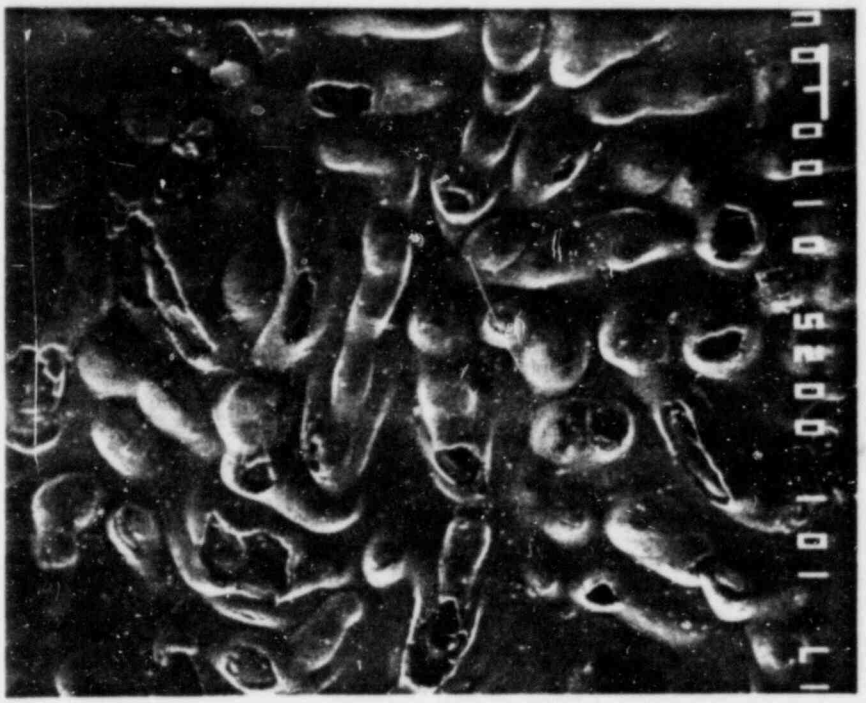

Figure 4. Blister formation and cracking in anatase films formed in Ti-Ti crevices exposed to WIPP Brine A for two weeks at 150°C. Magnification 100 X.

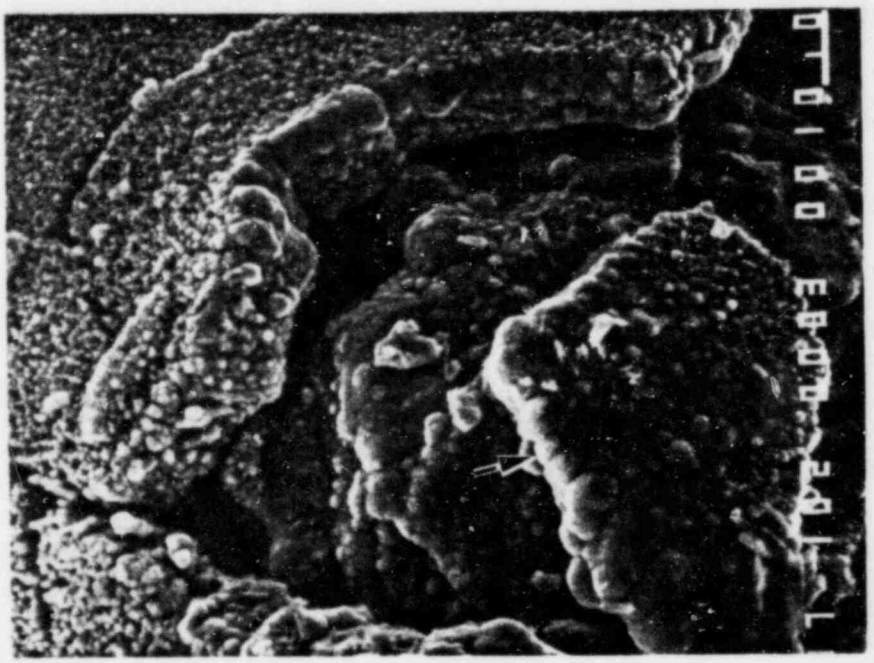

Figure 5. Anatase blister ruptured by hydrogen gas pressure during exposure of Ti-Ti crevices to WIPP Brine A for two weeks at 150°C. The arrow shows rutile crystals forming on the crack surfaces. Magnification 1000 X.

cracked blister with aggregates of rutile crystals forming on the crack surfaces. For samples showing lesser amounts of crevice corrosion, however, blisters were absent. Instead, the anatase transforms directly to rutile as shown in Figure 6. In this figure, the block-shaped crystals (top left) and the very large crystals are anatase. The rutile region is seen (bottom left) between the two large anatase islands. It is possible that anatase crystals transform to rutile before the solution pH and potential becomes low enough for the hydrogen evolution to become a cathodic reaction. This will be studied more fully in future work.

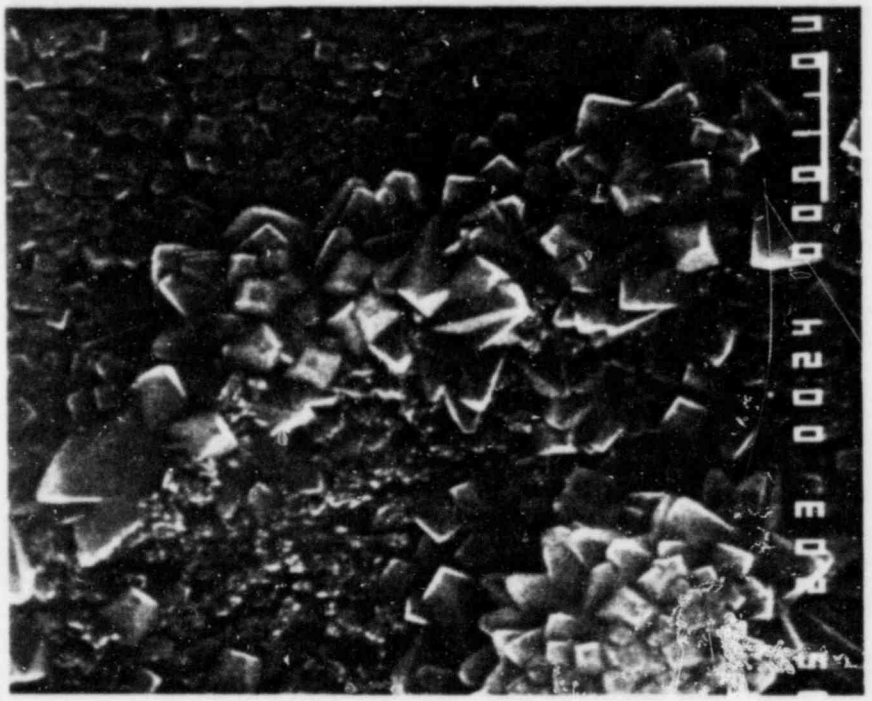

Figure 6. Transformation of rutile (bottom left) from anatase in Ti-Ti crevice samples exposed to WIPP Brine A for four weeks at 150°C. The block-shaped crystals and the large islands of large crystals are anatase. Magnification 20000 X.

Some experiments were also performed at 250°C. At this temperature, anatase transforms to Ti_3O_5 rather than to rutile, as shown in Figure 7. The micrograph shows mainly pointed anatase crystals with small clusters of Ti_3O_5 just beginning to form (bottom left). After transformation is complete, the block-type morphology of the Ti_3O_5 is apparent (Figure 8). Blister formation and cracking of the anatase scale is also observed at 250°C as shown in Figure 9.

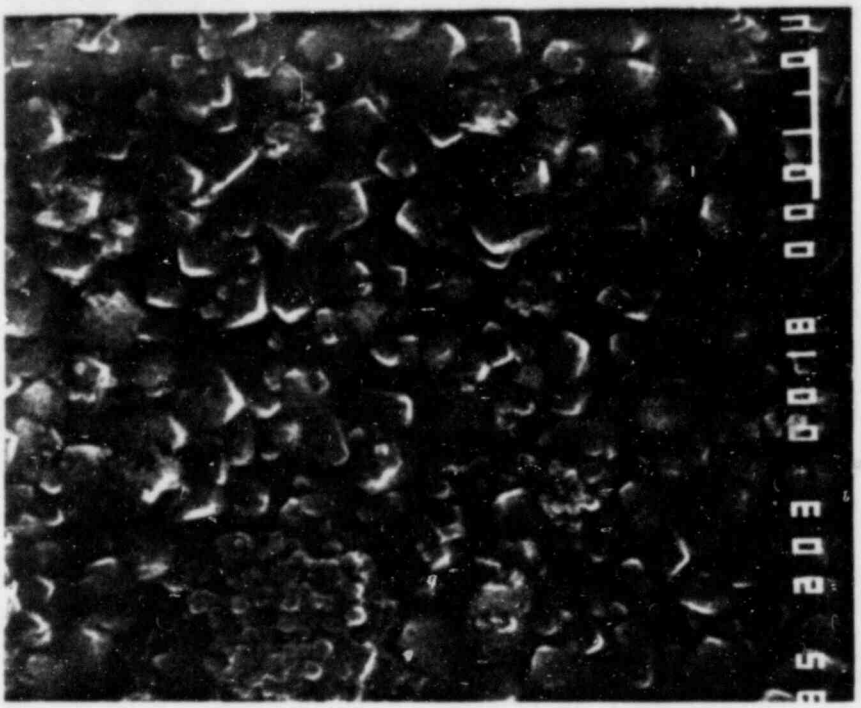

Figure 7. Ti_3O_5 crystals (small cluster, bottom left) transforming from anatase crystals after exposure of Ti-Ti crevices to WIPP Brine A for four weeks at 250°C. Magnification 20000 X.

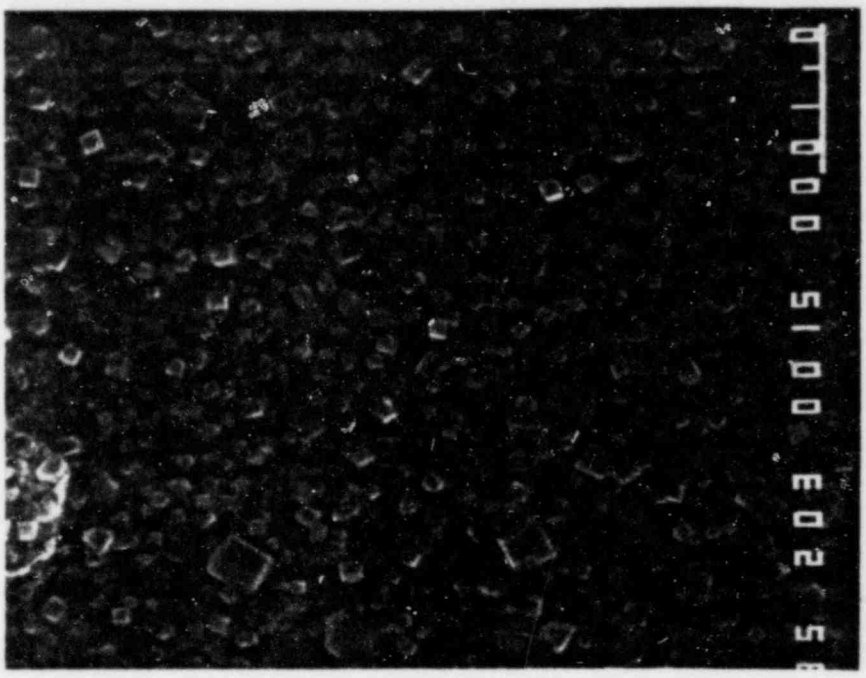

Figure 8. Ti_3O_5 crystals after transformation from anatase in Ti-Ti crevices exposed to WIPP Brine A at 250°C. Magnification 20000 X.

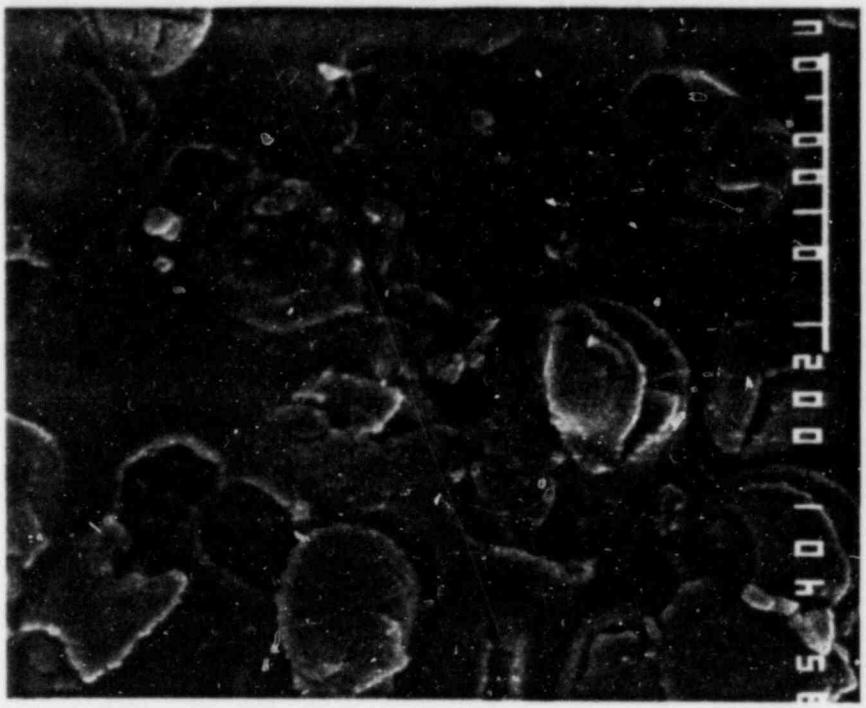

Figure 9. Cracking of anatase blisters by hydrogen pressurization in Ti-Ti crevices exposed to WIPP Brine A for four weeks at 250°C. Magnification 400 X.

Based on the above findings, the following mechanism is proposed for Ti-Ti crevice corrosion during exposure to brine at 150°C:

1. Dissolved oxygen inside the crevice decreases as it is absorbed by a cathodic reaction and the crevice gradually becomes an anode.

2. Anatase scale inside the crevice (the anode) grows faster than it does outside and the concentration of H^+ inside the crevice increases. Cl^- ions begin to migrate from the bulk solution into the crevice. Low pH accelerates the anatase scale growth rate and large anatase crystals are formed. At the same time, the potential inside the crevice decreases.

3. Because of the low potential inside the crevice, H_2 gas evolution becomes a cathodic reaction in this region. H_2 probably forms at the interface between the metal and anatase scale and may also form between anatase layers.

4. Owing to hydrogen formation beneath the anatase scale, blisters form by gas pressurization and when the pressure is sufficiently high the blisters fracture. Acidic solution enters the blister region and metal is dissolved as titanium ions.

5. A hydrolysis reaction occurs and TiO_2 precipitates around the cracks. Because of the low potential and low pH, rutile is more stable and grows on the surface of the anatase scale.

6. Hydride forms beneath the anatase scale and embrittles and disintegrates the metal.

At 250°C, however, Ti_3O_5 is the dominant oxide rather than rutile.

2. CORROSION OF TiCode-12

In this quarter, previous results were confirmed on TiCode-12 crevice corrosion in WIPP Brine A at 150°C. These were summarized in a paper and submitted for publication in the ASTM Special Technical Publication on Titanium and Zirconium in Industrial Applications (New Orleans, September 1982). Also a paper on the corrosion properties of TiCode-12 was submitted for publication in the proceedings of the Materials Research Society Meeting, (Boston, November 1982). The topics in this paper include crevice corrosion, hydrogen embrittlement, stress corrosion, and uniform corrosion of TiCode-12. All the data summarized are from previous BNL results. Draft copies of the two papers are given in Appendixes A and B.

3. HYDROGEN EMBRITTLEMENT OF TiCode-12

Preliminary data were reported in the last quarterly report[1] concerning the fracture properties of single-edged-notched (SEN) tensile specimens. At that time, the results on hydrogen concentration levels for all of the specimens were not available. In addition, no data were reported for as-received and vacuum degassed TiCode-12. In this reporting period a more complete series of tests was carried out, as summarized in Table 1. Figure 10 shows load-displacement curves for the specimens which were tested at room temperature. Previous BNL analyses showed that for as-received material the hydrogen concentration level is about 34 ppm. In the case of vacuum degassed (750°C, 5 hours) specimens, the hydrogen level measured for one sample was 4.5 ppm and for another 100 ppm. The latter high value may have resulted from contamination within the vacuum furnace or by error in the analytical procedure. This will be checked as soon as possible. However, the value of 4.5 ppm appears to be the more reasonable.

Hydrogen embrittlement may be identified in several ways including measurements of ductility loss, fracture toughness loss, and crack initiation energy. In a prior report[7] it was shown that TiCode-12 is susceptible to embrittlement for hydrogen levels of 6560 ppm and higher. This was concluded from fracture toughness evaluation. In the present lower range of hydrogen levels, fracture toughness procedures are less relevant because load-displacement curves are not as ideal as those specified in the ASTM standard.[8] A crack-initiation-energy approach is, therefore, being pursued in the current work using the data in Figure 10. Since the area beneath the load-displacement curve may be used as a measure of the crack initiation energy,[6]

Table 1

Tensile Testing Results for Hydrogenated TiCode-12

Sample	Hydrogen Concentration (ppm)	Macroscopic Fracture Morphology	Fractograph
1	7187	Flat	See Figure 11
2	892	Flat	See Figure 12
3	210	Flat and minor shear lip	See Figure 13
4	197	Flat and minor shear lip	See Figure 14
5 (vac. ann.)	4.5*	Shear lip	See Figure 15
6 (as-rec'd.)	34	Shear lip	See Figure 16

*Most likely value although a level of 100 ppm was also measured.

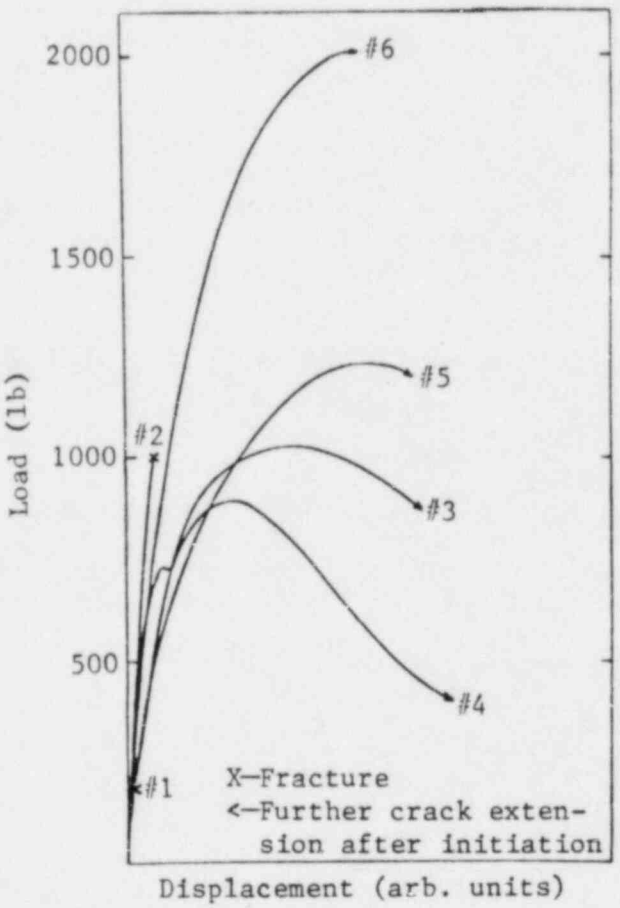

Figure 10. Load-displacement curves for TiCode-12 SEN samples containing various hydrogen concentration levels. The hydrogen levels for specimens 1 through 6 are 7187, 892, 210, 197, 4.5, and 34 ppm, respectively.

a simple correlation may be obtained relating embrittlement to hydrogen concentration. From Figure 10 it may be seen that as the hydrogen level is increased the energy for crack initiation decreases markedly; compare the areas beneath the curves for specimens 5 and 6 (vacuum degassed and as-received material, respectively) with those for specimens 3 and 4 (210, 197 ppm H_2), specimen 2 (892 ppm H_2), and specimen 1 (7187 ppm H_2). The discrepancy between the as-received and vacuum degassed specimens may be a result of (1) differences in microstructures, (2) oxygen or nitrogen concentration differences, or (3) hydrogen contamination. A study of these possibilities is underway.

At high hydrogen concentrations (7187 ppm) the fractograph in Figure 11 shows brittle interfacial separation and crystallographic fracture. When the hydrogen level is decreased to 892 ppm, crystallograpic fracture disappears and extensive subsurface transgrannular cracking is observed (Figure 12). Many of the cracks appear in dimpled ductile areas and may have formed during passage of the main crack front. Such behavior has been reported previously for a Ti-6Al-4V alloy.[9] For hydrogen levels of 197-210 ppm, the fracture surfaces show that failure occurs by a mixture of small cleavage areas and much larger regions displaying ductile microvoid coalescence features (Figures 13 and 14). The appearance of the latter is proof that for these hydrogen levels the failure mechanism is mainly ductile in nature. A similar type of mixed fracture behavior has been found for Ti-6Al-4V.[10] In the case of the as-received and vacuum degassed specimens, there is little difference in the fracture characteristics when compared to material containing approximately 200 ppm of hydrogen. Small amounts of cleavage are still present although microvoid coalescence is the principal fracture process (Figures 15 and 16).

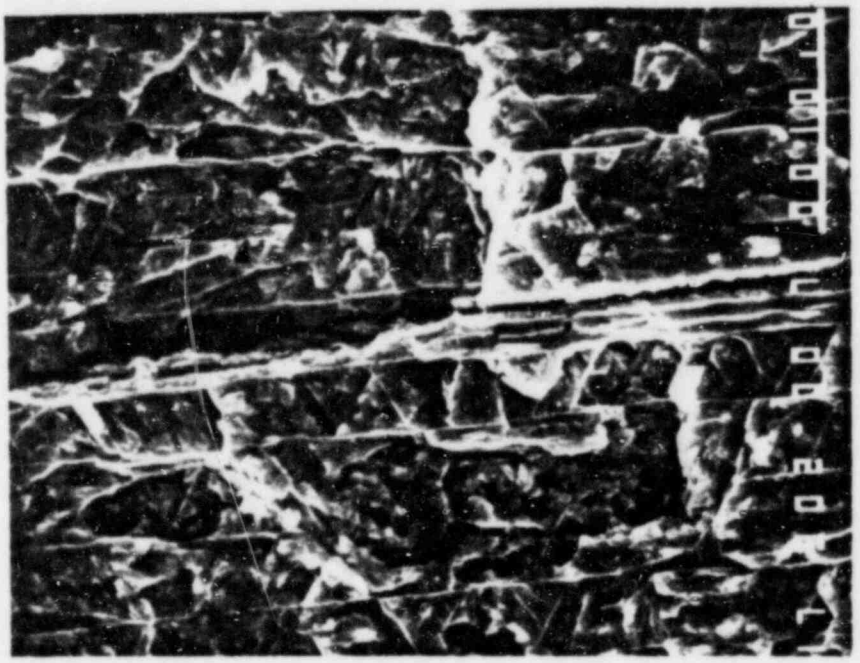

Figure 11. Brittle interfacial separation and crystallographic fracture in TiCode-12 at high hydrogen concentrations (7187 ppm). Magnification 9000 X.

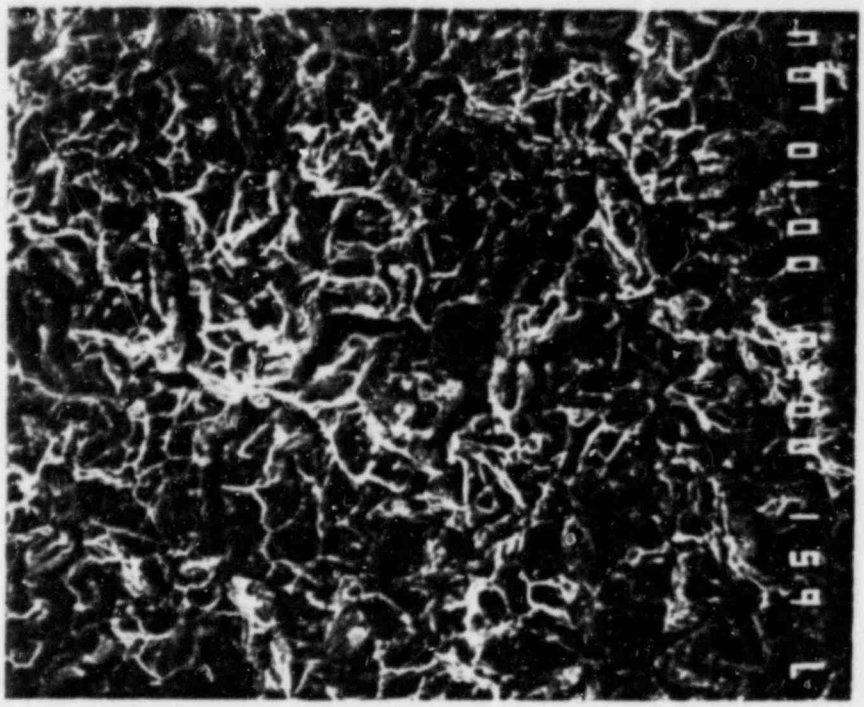

Figure 12. Subsurface transgranular cracking in TiCode-12 formed during passage of the main crack front at a hydrogen concentration of 892 ppm. Magnification 650 X.

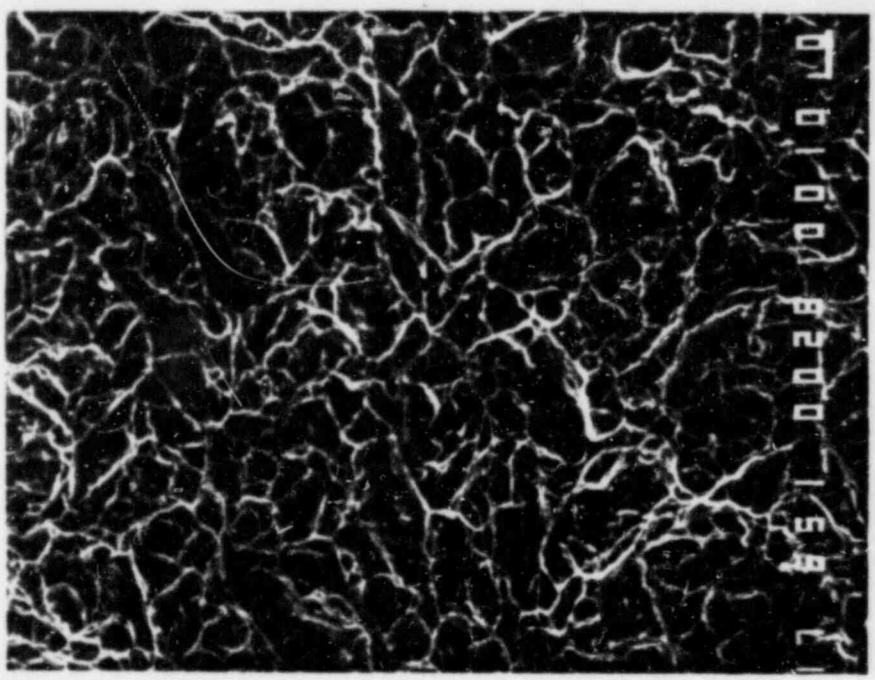

Figure 13. A mixture of small cleavage areas and much larger regions displaying ductile microvoid coalescence in TiCode-12 with a hydrogen concentration of 210 ppm. Magnification 650 X.

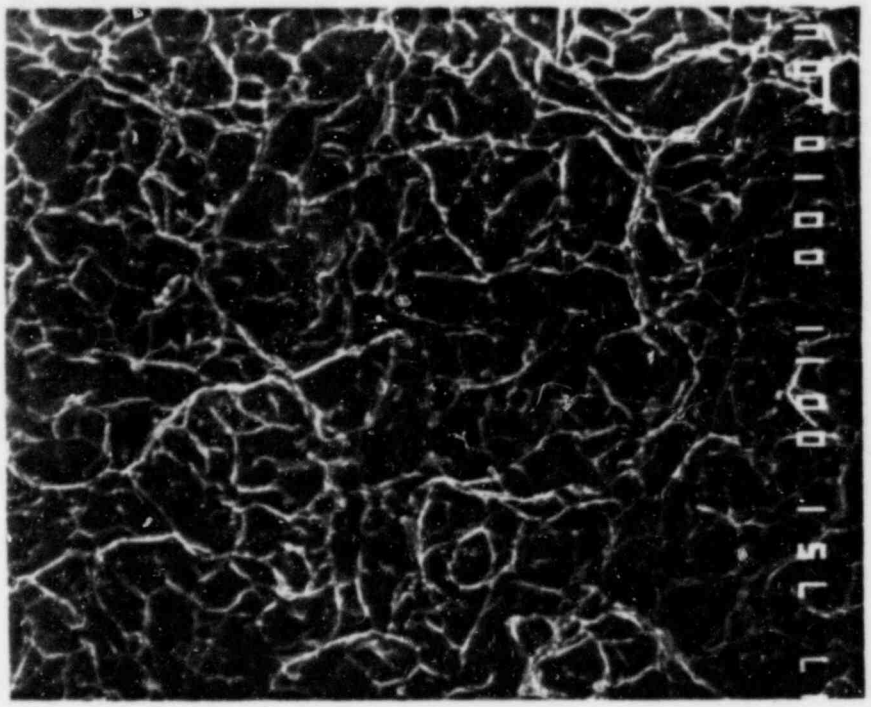

Figure 14. A mixture of small cleavage areas and much larger regions displaying ductile microvoid coalescence in TiCode-12 with a hydrogen concentration of 197 ppm. Magnification 750 X.

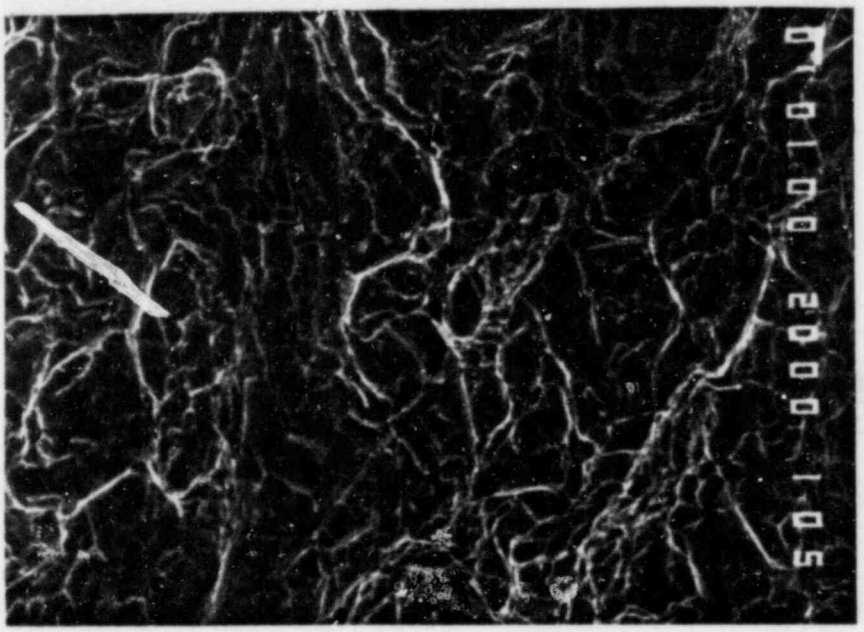

Figure 15. Fractograph of a vacuum annealed sample of TiCode-12. Small amounts of cleavage are still present although microvoid coalescence is the principal fracture process. There is no distinction between the vacuum annealed sample and those with a hydrogen concentration of about 200 ppm. Magnification 500 X.

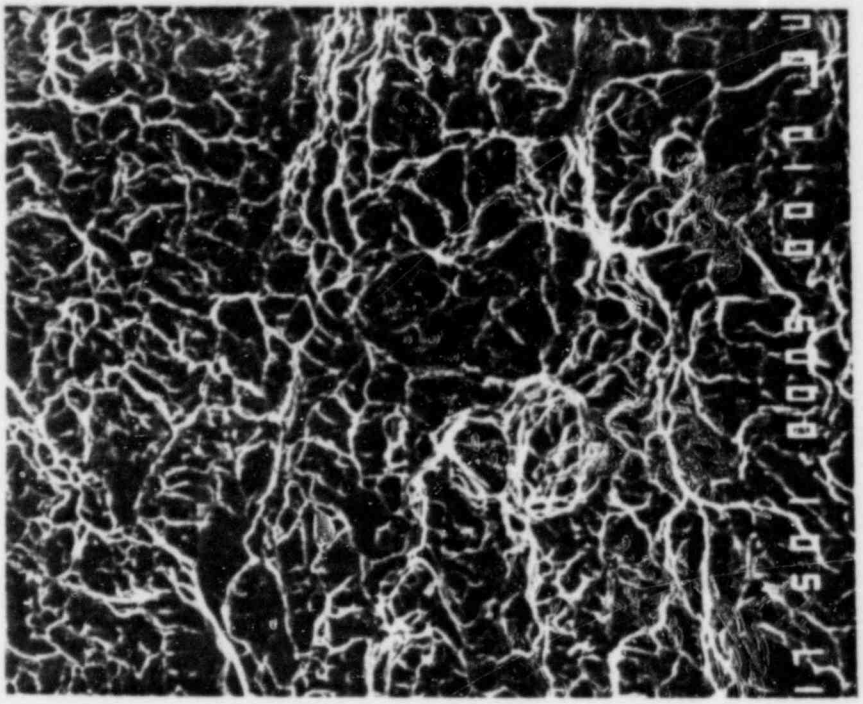

Figure 16. Fractograph of an as-received sample of TiCode-12 showing small amounts of cleavage and major microvoid coalescence. There is no distinction between the as-received sample, vacuum annealed sample, and samples with hydrogen concentrations of about 200 ppm. Magnification 500 X.

From the above observations it is concluded that TiCode-12 shows hydrogen embrittlement characteristics which are very similar to those observed for other near-alpha-phase alloys such as Ti-6Al-4V and Ti-6Al-6V-2Sn. Since these materials have been shown to fail by a hydride formation process[11] it is concluded that TiCode-12 fails by the same mechanism.

4. RADIATION EFFECTS

In the last quarterly report[5] preliminary results were given on the analysis of gases generated during the gamma radiolysis of WIPP Brine A. Unexpected products such as helium and CH_3OH were apparently detected and work was undertaken to check the data. It is possible that the methanol was introduced by incomplete drying of the irradiation capsule after cleaning, or during chemical analysis of the gas. In the case of the helium, this may have been introduced during the leak detection procedure used for the glass irradiation capsule. If it is assumed that the detection of the CH_3OH and helium are artifacts then the gas volumes specified previously may be simply adjusted to the values given in Table 2.

Table 2

Reanalysis of Gas Generated During Gamma Radiolysis of WIPP Brine A

Sample No.	Total Dose (rad x 10^{-8})	Pressure Percentage						
		H_2	O_2	N_2	CO_2	H_2O	Ar	$G(H_2)$
1-run 1	6.95	67.24	24.97	4.18	3.29	0.27	0.06	0.22
1-run 2	7.39	64.73	29.33	4.98	0.54	0.35	0.07	0.24
		66.09	27.39	5.53	0.49	0.44	0.05	0.24
2-run 1	3.55	52.30	12.64	25.86	8.35	0.51	0.33	0.18

Table 3

Preliminary Results of Solution Analysis of Gamma Irradiated WIPP Brine A

Sample No.	Total Dose (rad x 10-8)	Cl_2 (μg/ml)	H_2O_2 (μg/ml)	pH
1-run 1	6.95	0.32	2.25	6.41
1-run 2	7.39	0.23	1.07	6.71
2-run 1	3.55	0.59	N.D.<0.2	6.35

N.D.: Non-detectable.

Some preliminary solution analyses have been obtained on the irradiated WIPP Brine A. Table 3 shows that quantities of Cl_2 are produced, together with hydrogen peroxide. The Cl_2 is apparently a new discovery since recent work by Jenks[12] did not detect this gas. The amounts of H_2O_2 observed in the current studies are significantly lower than those detected by Jenks.[12] The pH of the solution did not significantly change during irradiation. Further work will confirm these preliminary data and attempts will be made to determine if ClO_3^- and ClO_4^- species are also present in the irradiated brine.

5. REFERENCES

1. E. G. Bohlmann and F. A. Posey, "Aluminum and Titanium Corrosion in Saline Waters at Elevated Temperatures," in Proceedings of the First International Symposium on Water Desalination, Washington DC, October 1965.

2. J. C. Griess, "Crevice Corrosion of Titanium in Aqueous Salt Solutions," Corrosion, 24, 96 (1968).

3. R. B. Diegle, "New Crevice Corrosion Test Cell," Mat. Perform. 21, 43 (1982).

4. N. D. Tomashov, G. P. Chernova, Y. S. Ruscol, and G. A. Ayuyan, "The Passivation of Alloys on Titanium Bases," Electrochemica Acta 19, 159 (1974).

5. T. M. Ahn and P. Soo, "Container Assessment - Corrosion Study of HLW Container Materials, Quarterly Progress Report, April-June 1982," BNL-NUREG-31611, 1982.

6. R. W. Hertzberg, Deformation and Fracture Mechanics of Engineered Materials, John Wiley and Sons, New York, 1976.

7. T. M. Ahn and P. Soo, "Container Assessment - Corrosion Study of HLW Container Materials, Quarterly Progress Report, January-March 1982," NUREG/CR-2317, Vol. 2, No. 1, BNL-NUREG-51449, June 1982.

8. Standard Test Method for Plane-Strain Fracture Toughness of Metallic Materials, ASTM E399-81 (1981).

9. H. G. Nelson, D. P. Williams, and J. E. Stein, "Environmental Hydrogen Embrittlement of an α-β Titanium Alloy: Effect of Microstructure," Met. Trans. 3, 469 (1972).

10. D. A. Meyn, "Effect of Hydrogen Content on Inert Environmental Sustained Load Crack Propagation Mechanisms of Ti-6Al-4V," in Environmental Degradation of Engineering Materials in Aggressive Environments, M. R. Louthan, Jr., R. P. McNitt, and R. D. Sission, Jr., Ed., VPI, Virginia, 1981.

11. N. R. Moody and W. W. Gerberich, "Hydrogen Induced Slow Crack Growth in Ti-6Al-6V-2Sn," Met. Trans. A. 11A, 973 (1980).

12. G. H. Jenks and J. R. Walton, "Radiation Chemistry of Salt-Mine Brines and Hydrates," ORNL-5726, 1982.

APPENDIX A

IDENTIFICATION OF CREVICE CORROSION IN THE TITANIUM ALLOY TiCode-12 IN SIMULATED ROCK SALT BRINE AT 150°C*

T. M. Ahn, B. S. Lee, and P. Soo
Brookhaven National Laboratory
Upton, NY 11973

*This work was carried out under the auspices of the U.S. Nuclear Regulatory Commission.

ABSTRACT: TiCode-12 (Ti - 0.3 Mo - 0.8 Ni) is a prime corrosion resistant material for high level nuclear waste containers which will be emplaced in mined geologic repositories such as those in rock salt. The crevice corrosion behavior of this alloy was investigated in simulated rock salt brine solutions at a temperature of 150°C. A distinct corrosion product with a range of interference colors was observed in a mechanically simulated crevice after two to four weeks' exposure. Low pH accelerated the reaction rate and deaerated solutions gave less corrosion than aerated ones. Also, increasing specimen size, decreasing crevice gap, and preoxidation of the cathodic area gave more voluminous corrosion products inside the crevice. High temperature did not necessarily accelerate crevice corrosion. These results are consistent with those expected from macroscopic concentration cell formation accompanied by oxygen depletion, potential drop, and acidification inside the crevice. TEM and SEM techniques were extensively utilized to identify the film formed inside the crevice at each stage of the corrosion process. In the early stage of cell formation, compact anatase-type TiO_2 was formed which acted as a barrier to further corrosion inside the crevice. Traces of Ti_3O_5 were also identified. In the case of severe crevice corrosion, the corrosion product was identified as a porous rutile form of TiO_2. Measurements of the open circuit corrosion potentials at 80°C showed that there is a breakdown of the passive film as the pH of the brine falls below unity. Accelerated hydrogen uptake was observed in the crevice region. This was caused by breakdown of the passive film or by high acidity in the crevice. Based on these observations, and pH and potential measurements inside the crevice of commercially pure titanium done by other workers, a mechanism for crevice corrosion in TiCode-12 has been developed. It involves the initial formation of compact

anatase crystals inside the crevice. As the macroscopic cell develops further, it is postulated that either the anatase form of TiO_2 will transform to the lower oxide Ti_3O_5 and to the rutile form of TiO_2, or titanium dissolves into the solution after the breakdown of the protective film and subsequent hydrolysis takes place to form the lower oxide and the rutile form of TiO_2. The role of alloying elements (Mo and Ni) and dissolved solutes are discussed with respect to these postulations.
KEY WORDS: TiCode-12, brine, crevice corrosion, anatase, rutile.

Introduction

There is currently in the U.S.A. an effort to develop titanium alloy TiCode-12 (Ti - 0.3 Mo - 0.8 Ni) as a prime corrosion resistant material for high level nuclear waste containers which will be emplaced in mined geologic repositories such as those in rock salt [1-7]. Crevice-type environments are expected to form between the TiCode-12 container and surrounding backfill materials or metallic emplacement sleeves. Earlier screening tests of various candidate materials showed that TiCode-12 is immune to crevice corrosion in simulated rock salt brines (neutral pH) below the temperatures of 300°C and dissolved oxygen concentrations below 250 ppm [1]. This immunity has been attributed to the addition of Mo and Ni to titanium [8] since pure titanium shows significant crevice corrosion in neutral brines at 150°C or below [9,10]. This paper outlines the results of immersion tests, and electrochemical and surface analysis studies. The main objectives were to determine whether crevice corrosion is likely in TiCode-12 exposed to simulated rock salt brines at 150°C and to ascertain the probable mechanisms involved.

Materials and Test Environments

TiCode-12 is a two-phase material composed of alpha and a minor beta phase. Sheet materials were obtained from TIMET Corporation. The nominal compositions are shown in Table 1. Small differences in the compositions were found by BNL in the analysis of Ni, Mo, and Fe in the various heats of TiCode-12 compared to those specified by the vendor. However, compositions were within specification.

TABLE 1--Nominal compositions of TiCode-12 (weight percent)

Ni	Mo	Fe	C	H	N	O	Ti
0.80	0.30	0.3M[a)]	0.1M	0.015M	0.03M	0.25M	Balance

[a)]M denotes the maximum.

Brine solutions selected for this study were based on those used by Sandia National Laboratories [1] which are considered to simulate those at the Waste Isolation Pilot Project Site in New Mexico. The concentrations of the major ions in the solutions used are shown in Table 2. The majority of the work was performed on Brine A and the main test temperature was 150°C.

TABLE 2--Compositions of brine solutions (ppm) [1]

Brine	Na^+	K^+	Mg^{+2}	Ca^{+2}	Sr^{+2}	Cl^-	SO_4^{-2}	I^-	HCO_3^-	Br^-	BO_3^-
A	42000	30000	35000	600	5	190000	3500	10	700	400	1200
B	11500	15	10	900	15	175000	3500	10	10	400	10

Experimental Procedures

Three different sizes of coupons were used (1 x 2, 2 x 2, and 2 x 4 cm) for the tests on crevice corrosion. After mirror polishing of the coupons up to 6 μm diamond paste, a crevice was simulated by joining metal/metal or metal/Teflon couples with titanium bolts. The immersion studies were performed in quartz tubes or in static autoclaves for two to four week periods. The acidity and oxygen concentration of the solutions were varied. The degree of corrosion was examined optically and the morphology of the corrosion product inside the crevice was analyzed by SEM. An oxide film sample from

inside the crevice was selected by punching out an area of diameter 3.2 mm from the coupon. The oxide was carbon coated and it was stripped off chemically by etching (etchant: 2% HF solution). It was identified by TEM diffraction analysis.

In order to obtain kinetic data on the effect of acidified brine on the passivation behavior, the open circuit corrosion (o/c) potential behavior was examined at 80°C for Brine A. Pre-electrolysis of the solution was used to obtain a brine redox potential close to that expected from the ionic concentrations. Also, the surface of the sample was anodized after polishing with 600-grit SiC paper to minimize the influence of the air formed oxide film.

Hydrogen uptake experiments were performed in Brine B during immersion tests on single and creviced coupons at 150°C in an autoclave with a hydrogen overpressure at room temperature of 1.5 MPa. Passivity breakdown or low pH will lead to enhanced hydrogen uptake because of high proton concentration or the easy dissociation of hydrogen molecules into atoms on the pristine titanium surface.

Results

During the initial stage of crevice corrosion (first few days of immersion), a very thin multicolored corrosion product was observed. This type of film was found especially in smaller samples and remained for exposures greater than two weeks. Three distinctive areas (blue, violet, and yellow regions) were selected for electron diffraction. Regardless of the color, the diffraction patterns showed strong anatase TiO_2 peaks. Traces of Ti_3O_5 were also identified. The anatase form of TiO_2 was mostly present

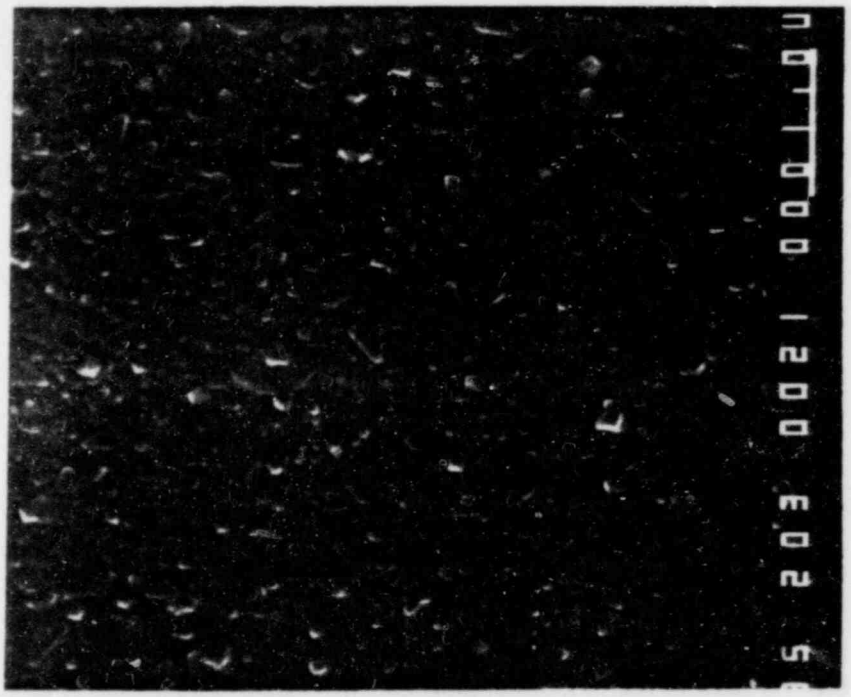

FIGURE 1--SEM micrograph of the anatase form of TiO_2. Magnification 20000 X.

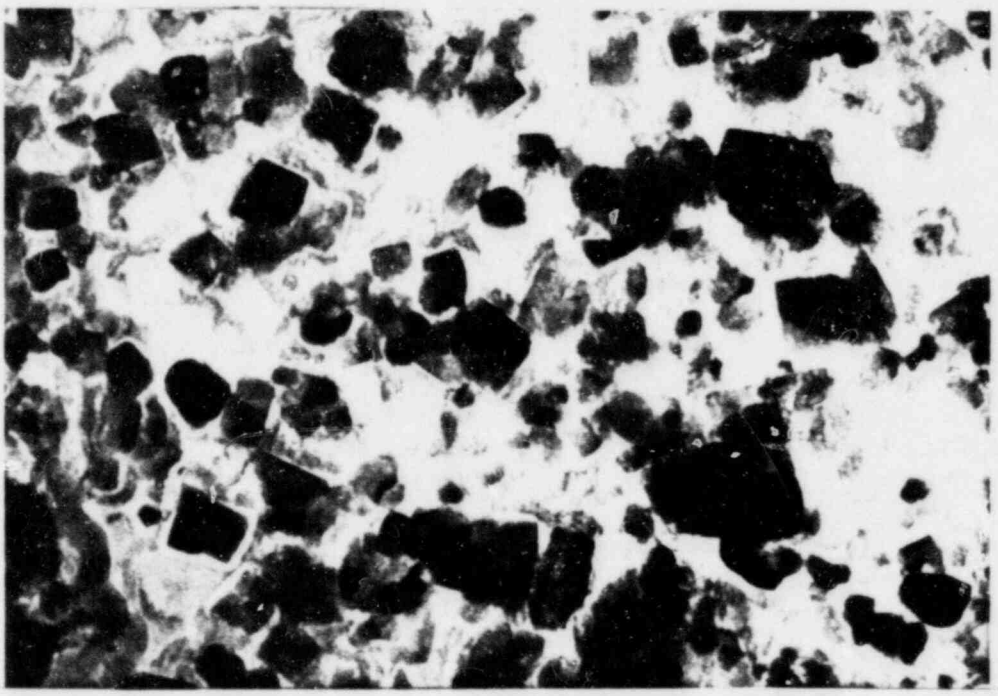

FIGURE 2--TEM micrograph of the anatase form of TiO_2. Magnification 200000 X.

as block-shaped crystals as shown in Figures 1 and 2. For exposures of over two weeks, the largest samples (2 x 4 cm) with the smaller crevice gaps showed severe black corrosion products. This was composed of the rutile form of TiO_2 with traces of lower oxide also present. The rutile was in the form of needle-shaped crystals as shown in Figures 3 and 4.

The severest attack was observed when the sample size was increased as described previously. Metal/Teflon crevice corrosion was more severe than that for metal/metal crevices. Aerated solutions gave more severe attack than deaerated solutions, and lower pH enhanced the crevice corrosion rate. In addition, preoxidation of the cathodic area gave more voluminous corrosion products. A typical example of severe attack is shown in Figure 5. However, increasing temperature did not necessarily accelerate the corrosion rate. At 250°C, for two to four weeks' exposure, no severe attack was observed.

In acidified Brine A (pH = 1), the o/c potential attained a value of -360 mV sce after discontinuing anodic polarization as shown in Figure 6. After approximately four hours' immersion, the potential reached a value of ~-550 mV sce, and did not change appreciably during the remainder of the test. In the time taken to attain the steady state condition, evidence of potential excursions was observed. Since titanium is passive in 1 M acidified chloride solutions (pH=1) for potentials greater than ~-300 mV sce [9,11], this o/c behavior indicates that there is sporadic breakdown of the passive film.

Table 3 shows hydrogen uptake results for tests lasting 14 days. The crevice samples show significantly higher hydrogen concentrations than those for the single coupons.

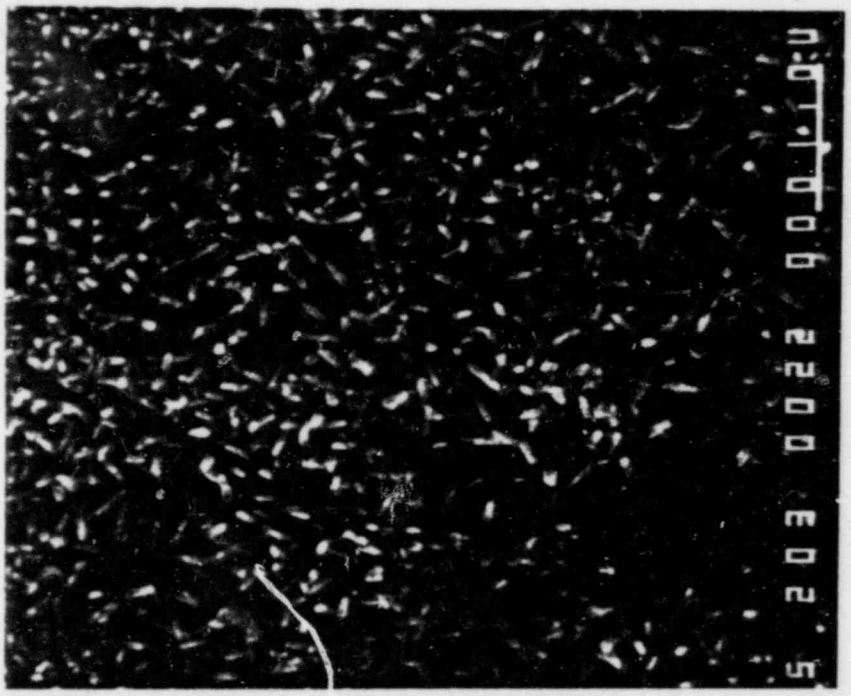

FIGURE 3--SEM micrograph of the rutile form of TiO_2. Magnification 20000 X.

FIGURE 4--TEM micrograph of the rutile form of TiO_2. 200000 X.

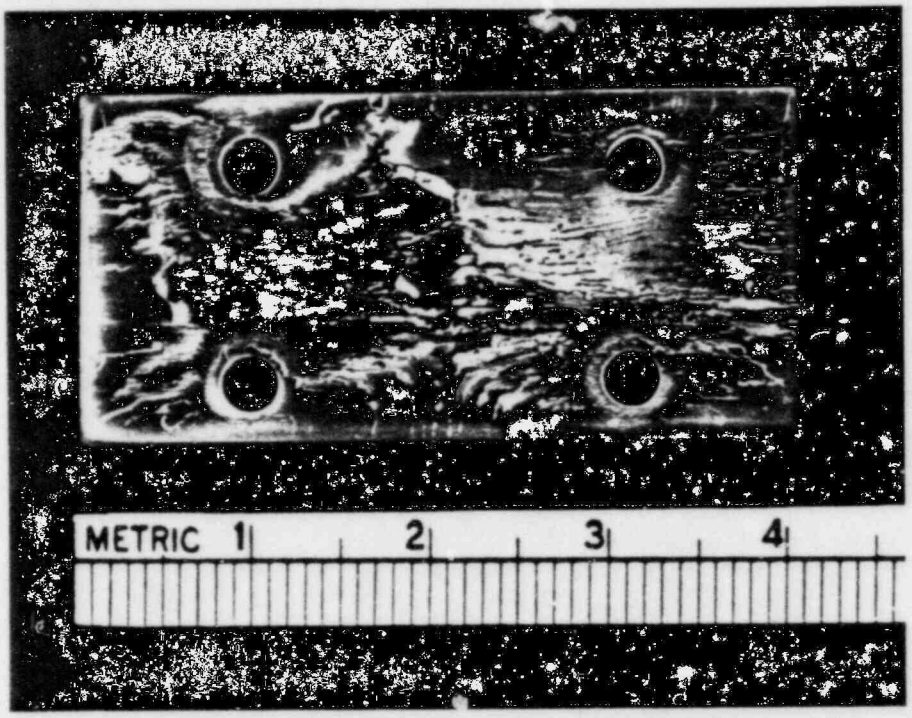

Severe attack

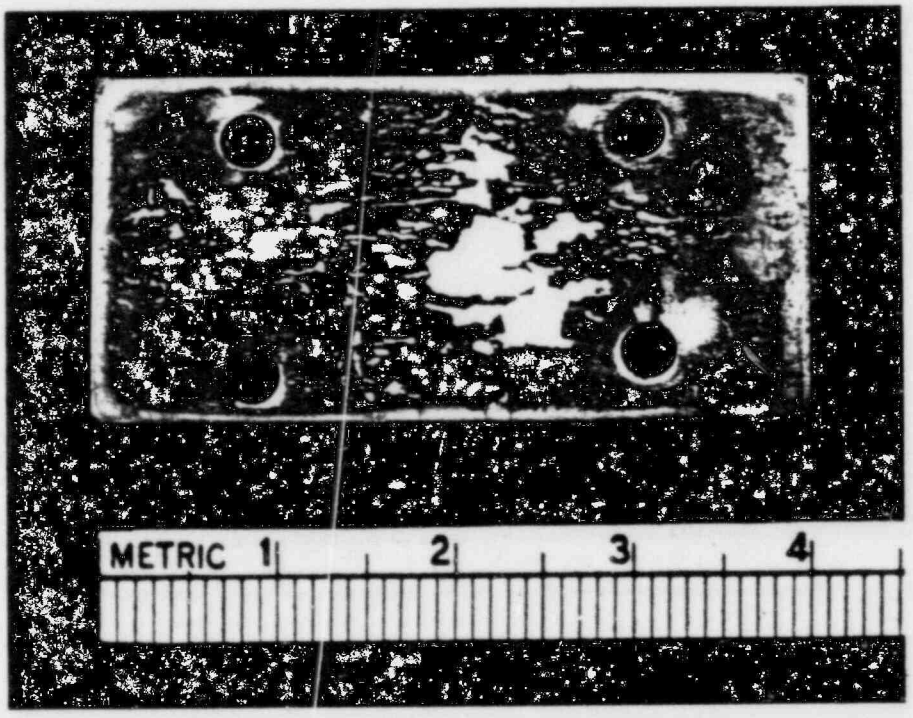

Initial stage of attack

FIGURE 5--Optical micrographs of severe crevice corrosion and the initial stage of attack.

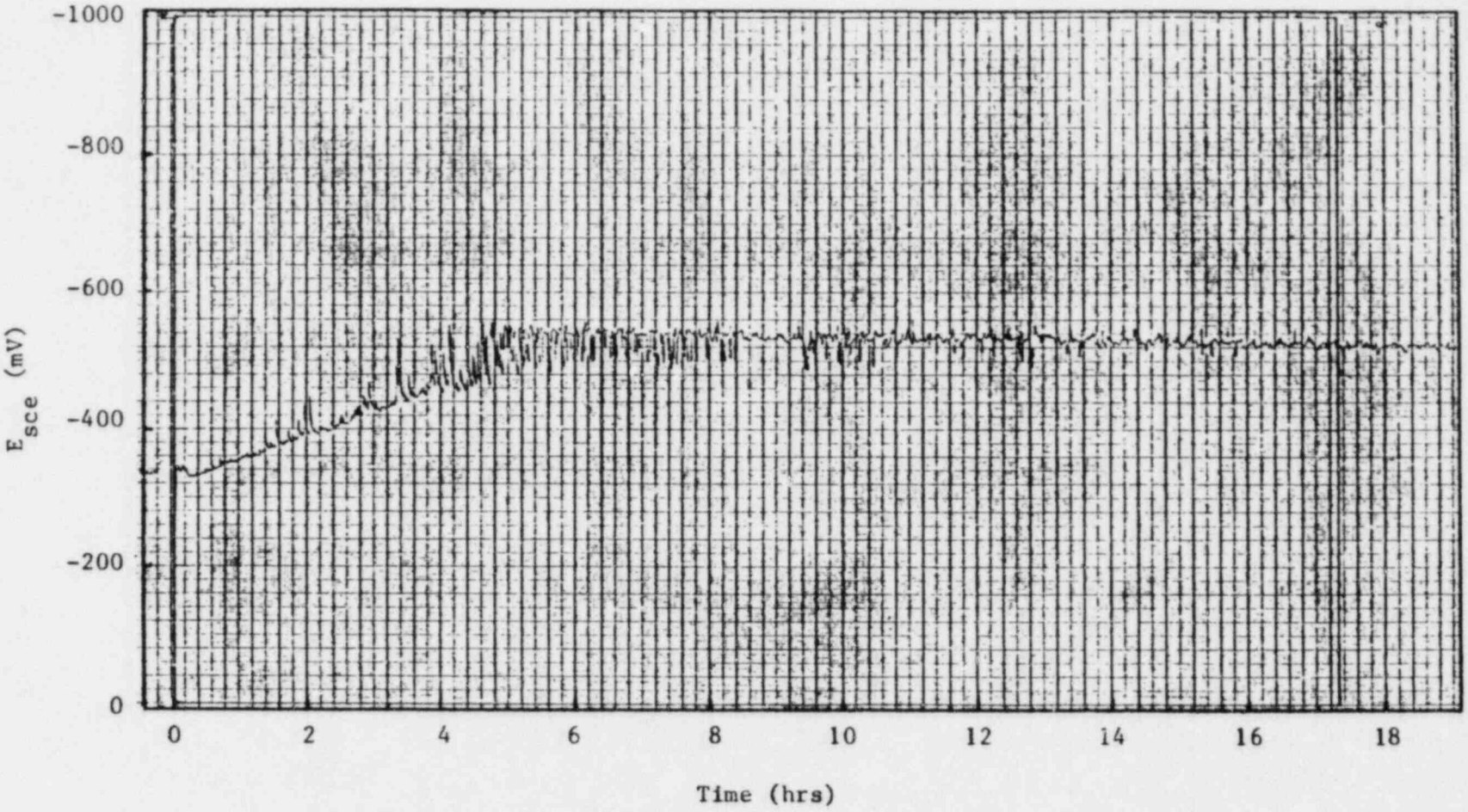

FIGURE 6-- Open-circuit corrosion potential of TiCode-12 in 1 M acidified Brine A at 80°C.

TABLE 3--Hydrogen uptake results (ppm) for TiCode-12 in Brine B for 14 days

Run	Single Coupon	Crevice Samples	
1	65.8	80.6	91.2
2	32.5	74.4	

Note: The hydrogen concentration is 34 ppm in the as-received sample.

Discussion

It is evident that the formation of a concentration cell is responsible for crevice corrosion. The concentration of oxygen inside the crevice compared to the bulk solution will determine the severity of corrosion for the initial aeration cell. The results for aerated solutions showed this effect quite clearly. Also, increasing the sample size and decreasing the crevice gap (metal/Teflon samples) gives lower oxygen (or other species) inflow into the center of the crevice, leading to more severe crevice corrosion. These observations are consistent with the results of a mass balance calculation of oxygen concentrations inside the crevice [12]. Temperature effects may also be explained on the basis of the above arguments. Above a certain critical temperature, the diffusion rates of any species are so fast that a concentration cell may not develop easily thereby minimizing crevice attack.

The results obtained on the effect of surface preoxidation are an indication of potential drop occurring inside the crevice. The preoxidation probably decreases the cathodic reaction rate facilitating a potential drop inside the crevice. Similar behavior was noted by Diegle who observed a potential drop in a Grade 2 titanium crevice specimen exposed to acidified chloride-containing solutions at 150°C [13].

The data on solution pH effects implies that it is necessary to attain very low pH values to cause severe crevice corrosion in TiCode-12. This confirms earlier work on the crevice corrosion of CP titanium in concentrated neutral brine solutions at 150°C [9]. The pH drop and passivity breakdown are consistent with the results on o/c potential behavior and hydrogen uptake since high acidity and a pristine surface will enhance hydrogen uptake [14].

In the literature, three different oxide forms have been reported as possible corrosion products of titanium and its alloys in acidic solution [15,16] or in neutral NaCl solutions [9,17]. These are the stable rutile form of TiO_2 (a tetragonal crystal structure), the metastable anatase form of TiO_2 (a tetragonal crystal structure), and another metastable brookite form of TiO_2 (an orthorhombic crystal structure). Metastable forms have been reported to act as a barrier to corrosion and drastically slow down the corrosion proces [15]. However, the rutile form is known to be porous (Figures 3 and 4) and it causes accelerated attack. Figures 7-9 show the sequence of rutile formation within the crevice. Initially, rutile needles are formed on the anatase surface (Figure 7) forming domains (Figure 8). The thick rutile in these areas is often cracked as shown in Figure 9. Cracking was not observed in the anatase phase for TiCode-12 but in a related test in commercial purity titanium severe anatase cracking was noted (Figure 10). With respect to the mechanism of rutile formation it is not currently clear whether it forms by the transformation of the anatase via lower oxides, or whether it is formed by the reprecipitation of metal ions in solution.

TiCode-12 is a dilute alloy of titanium containing small additions of Mo and Ni. Depending on the amount of these elements, the degree of active

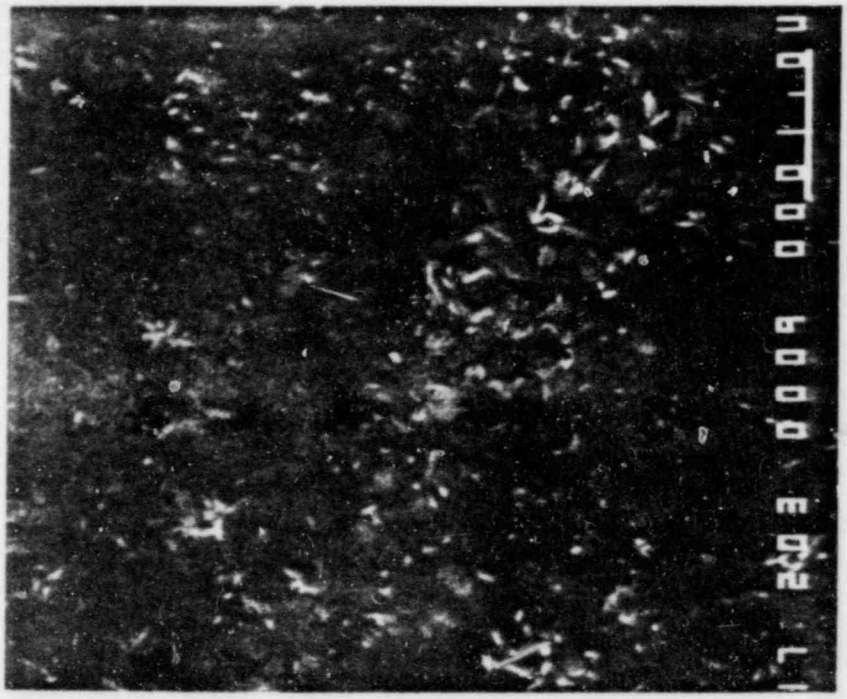

FIGURE 7--Initial stage of rutile formation.
Magnification 20000 X.

FIGURE 8--Growing rutile islands.
Magnification 2000 X.

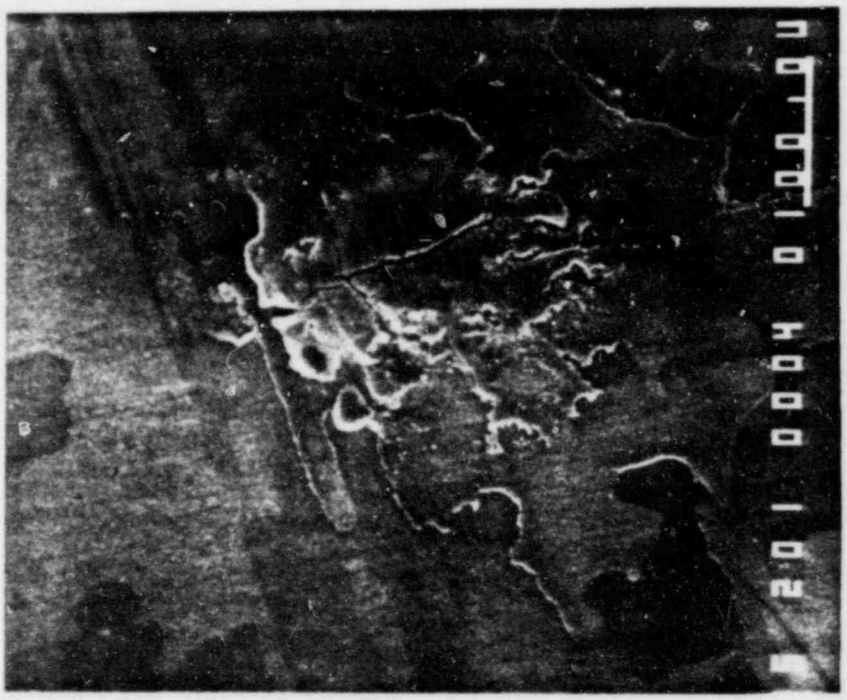

FIGURE 9--Well-developed rutile scale showing mechanical breakdown of the scale. Magnification 200 X.

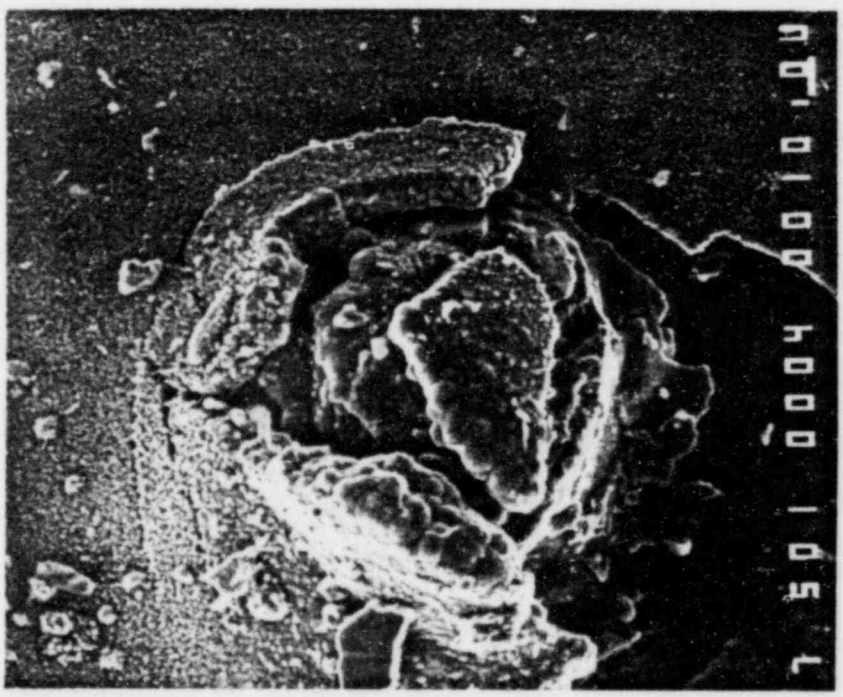

FIGURE 10--The mechanical breakdown of the anatase form of TiO_2 in commercially pure titanium. Magnification 500 X.

dissolution is known to vary [9]. Our experiments show that TiCode-12 is very resistant to crevice corrosion compared to commercially pure titanium [12]. Often these alloying elements cause active/passive cyclic behavior [9]. The fluctuations observed in the o/c potential measurements may arise from this cyclic behavior which may be caused by the enrichment of Mo and Ni on the surface and subsequent dissolution of these elements. The details of the role of Mo and Ni are not known. Despite this sporadic behavior, the main passivity considerations discussed previously are believed to be of more importance with respect to crevice corrosion.

The halide (especially chloride) ion concentration is of lesser importance in crevice corrosion than the hydrogen ion activity [9]. However, Griess [9] does consider that the actual salt concentration is significant, i.e., the more concentrated the salt, the more severe the attack, irrespective of the halide ion. This behavior was observed in the present study. While the o/c potential shows spontaneous passivation in 0.1 M HCl and 0.9 M KCl (pH=1) [12], the present acidified Brine A causes breakdown of passivity with a chloride concentration of 5.35 M. The results on Brine B are similar to those for Brine A. This implies that the total salt concentration may be more important than the amounts of various types of salt.

Conclusions

Crevice corrosion of TiCode-12 was identified at 150°C in simulated rock salt brine solutions. Lower pH accelerated the reaction rates and deaerated solutions gave less corrosion than aerated ones. Also, increasing specimen size, decreasing crevice gap, and preoxidation of the cathodic area gave

more voluminous corrosion products. These results are consistent with those expected from macroscopic concentration cell formation accompanied by oxygen depletion, potential drop, and acidification inside the crevice. The results of oxide film analysis show that the compact anatase crystals are formed initially inside the crevice. As the macroscopic cell develops further, it is postulated that either the anatase form of TiO_2 will transform to the lower oxide Ti_3O_5 and to the rutile form of TiO_2, or titanium dissolves into the solution after the breakdown of the protective film and subsequent hydrolysis takes place to form the lower oxide and the rutile form of TiO_2.

Acknowledgments

Our thanks to G. Spira for general technical assistance, J. Woodward for the initial test of corrosion potential measurement, and M. McNeil (NRC) for program coordination.

References

[1] Braithwaite, J. W., Maganani, and J. W. Munford, "Titanium Alloy Corrosion in Nuclear Waste Environments," SAND79-2023C, 1979.

[2] Braithwaite, J. W. and N. J. Magnani, "Nuclear Waste Canister Corrosion Studies Pertinent to Geologic Isolation," Nuclear and Chemical Waste Management, Vol. 1, 1980, p 37.

[3] Molecke, M. A., D. W. Schaefer, R. S. Glass, and J. A. Ruppen, Sandia HLW Canister/Overpack Studies Applicable to Salt Repository," SAND81-1585, 1981.

[4] Westerman, R. E., "Investigation of Metallic, Ceramic, and Polymeric Materials for Engineered Barrier Applications in Nuclear Waste Packages," PNL-3484, 1980.

[5] Pitman, S. G., "Investigation of Susceptibility of Titanium-Grade 2 and Titanium-Grade 12 to Environmental Cracking in a Simulated Basalt Repository Environment," PNL-3914, 1981.

[6] Dayal, R., et al., "Nuclear Waste Management Technical Support in the Development of Nuclear Waste Form Criteria for the NRC, Task 1: Waste Package Overview," NUREG/CR-2333, Vol. 1, BNL-NUREG-51458, 1982.

[7] Ahn, T. M., et al., "Nuclear Waste Management Technical Support in the Development of Nuclear Waste Form Criteria for the NRC, Task 4: Test Development Review," NUREG/CR-2333, Vol. 4, BNL-NUREG-51458, 1982.

[8] Metals Handbook, Vol. 3, Ninth Edition, ASM, Metal Park, OH, 1980, p. 381.

[9] Griess, J. C. Jr., "Crevice Corrosion of Titanium in Aqueous Salt Solutions," Corrosion-NACE, Vol. 24, 1968, p. 96.

[10] Jackson, J. D. and W. K. Boyd, "Crevice Corrosion of Titanium," Applications Related Phenomena in Titanium Alloys, ASTM STP, Vol. 43, 1968, p. 218.

[11] Kelly, E. J., "Anodic Dissolution and Passivation of Titanium in Acidic Media," J. Electrochemical Soc., Vol. 126, 1979, p. 206.

[12] Ahn, T. M. and P. Soo, "Container Assessment - Corrosion Study of HLW Container Materials, Quarterly Progress Report, July-September 1981, October-December 1981, January-March 1982, April-June 1982," NUREG/CR-2317, BNL-NUREG-51449, Vol. 1, No. 3 and No. 4, Vol. 2, No. 1 and No. 2, 1982.

[13] Diegle, R. B., "New Crevice Corrosion Test Cell," Materials Performance, Vol. 21, 1982, p. 43.

[14] Covington, L. C. and N. G. Feige, "A Study of Factors Affecting the Hydrogen Uptake Efficiency of Titanium in Sodium Hydroxide Solutions," in Localized Corrosion - Cause of Metal Failure, ASTM STP 516, p. 222, 1971.

[15] Tomashov, N. D., G. P. Cernova, Y. S. Ruscol, and G. A. Ayuyan, "The Passivation of Alloys on Titanium Bases," Electrochemica Acta, Vol. 19, 1974, p. 159.

[16] Koizumi, T. and T. Nakayama, "Structure of Oxide Films Formed on Titanium in Boiling Dilute H_2SO_4 and HCl," Corrosion Science, Vol. 8, 1968, p. 195.

[17] Shreir, L. L., "Localized Corrosion," Corrosion, Vol. 1, L. L. Shreir, Ed., Newnes-Butterworths, 1979.

APPENDIX B

To be presented at the Annual Meeting of the Materials Research Society, Boston, Massachusetts, November 1-4, 1982.

BNL-NUREG-31876

CORROSION OF TiCode-12 IN A SIMULATED WASTE ISOLATION PILOT PROJECT (WIPP) BRINE*

T. M. AHN, B. S. LEE, J. WOODWARD, R. L. SABATINI, AND P. SOO
Brookhaven National Laboratory, Upton, NY 11973

ABSTRACT

The corrosion behavior of TiCode-12 (Ti-0.3 Mo-0.8 Ni) high level nuclear waste container alloy has been studied for a simulated WIPP brine at a temperature of 150°C or below. Crevice corrosion was identified as a potentially important failure mode for this material. Within a mechanical crevice, a thick oxide film was found and shown to be the rutile form of TiO_2, with a trace of lower oxide also present. Acidic conditions were found to cause a breakdown of the passive oxide layer. Solution aeration and increased acidity accelerate the corrosion rate. In hydrogen embrittlement studies, it was found that hydrogen causes a significant decrease in the apparent stress intensity level in fracture mechanics samples. Hydride formation is thought to be responsible for crack initiation. Stress corrosion cracking under static loads was not observed. Attention has also been given to methods for extrapolating short term uniform corrosion rate data to extended times.

INTRODUCTION

Currently in the U.S.A. there is an effort to develop titanium alloy TiCode-12 (Ti-0.3 Mo-0.8 Ni) as a prime corrosion resistant material for high level nuclear waste containers which will be emplaced in mined geologic repositories [1-7]. Preliminary data indicate that although uniform corrosion is unlikely to present a problem with respect to failure of the container, little information is available on possible localized corrosion failure mechanisms. The assessment of localized corrosion mechanisms is, therefore, essential for the prediction of the life time of the containers. This paper outlines initial results on the possible major localized failure modes of TiCode-12 in simulated rock salt brine solutions. Emphasis was on the study of crevice corrosion and hydrogen embrittlement. Crevice-type environments are expected to form between the TiCode-12 container and surrounding backfill materials or metallic emplacement sleeves. Hydrogen embrittlement is also possible since this material typically contains 30 ppm of hydrogen as a residual element. Furthermore, radiolysis of the groundwater may cause an increase in the hydrogen level. Preliminary results on stress corrosion cracking (SCC) are presented. Attention has also been given to methods for extrapolating short term uniform corrosion rate data to extended times, in order to predict container performance.

*This work was performed under the auspices of the U.S. Nuclear Regulatory Commission.

MATERIALS AND ENVIRONMENT

TiCode-12 is a two-phase material composed of alpha and minor beta phases. Plate and sheet materials were obtained from three different sources: RML, Timet, and Crucible. The nominal compositions are shown in Table I. Differences in the compositions were found by BNL in the analysis of Ni, Mo, and Fe in the various heats of TiCode-12. The maximum variation was a factor two larger than values specified by the vendors.

TABLE I
Nominal compositions of TiCode-12 (weight percent)

Ni	Mo	Fe	C	H	N	O	Ti
0.80	0.30	0.3M[a)]	0.1M	0.015M	0.03M	0.25M	Balance

a)M denotes the maximum.

Brine solutions selected for this study were based on those used by Sandia National Laboratories [1] which are considered to simulate salt repository conditions at the Waste Isolation Pilot Plant site. The concentrations of the major ions in the two solutions used are shown in Table II. The majority of the work was performed on Brine A. The reference text temperature was 150°C. Lower temperatures were sometimes used to develop an understanding of the mechanisms of failure.

TABLE II
Compositions of brine solutions (ppm) [1]

Brine	Na^+	K^+	Mg^{+2}	Ca^{+2}	Sr^{+2}	Cl^-	SO_4^{-2}	I^-	HCO_3^-	Br^-	BO_3^-
A	42000	30000	35000	600	5	190000	3500	10	700	400	1200
B	11500	15	10	900	15	175000	3500	10	10	400	10

EXPERIMENTAL PROCEDURES

Three different sizes of coupon were used (1 x 2, 2 x 2, and 2 x 4 cm) for the tests on crevice corrosion. After mirror polishing of the coupons, a crevice was simulated by joining metal/metal or metal/Teflon couples with titanium bolts. The immersion studies were performed in quartz tubes or in static autoclaves for two to four week periods at 150°C. The solution acidity and oxygen concentration of the solutions were varied. The degree of corrosion was examined optically and the corrosion products were analyzed by SEM and TEM.

Hydrogen embrittlement was evaluated at room temperature using thermally hydrogenated single-edged-notched (SEN) tensile samples [8] (cross head speed 0.005 cm/min) to determine the susceptibility of TiCode-12 to hydrogen embrittlement and to ascertain the probable mechanisms involved. The hydrogen concentration was determined after the tests by the vacuum extraction method and the fracture surface was examined by SEM. Hydrogen uptake experiments were

performed in Brine B during immersion tests on single and creviced coupons at 150°C in an autoclave with a hydrogen overpressure at a room temperature of 1.5 MPa (220 psi).

In the SCC study, both notched and un-notched C-rings were designed following ASTM standards [9] and these were loaded and sealed in quartz tubes containing acidified brines (pH = 1.1) to simulate crevice conditions. The test was performed at 150°C for an exposure time of three months. The acidified brine was also used in an attempt to understand the passivation behavior of TiCode-12. The open circuit corrosion potential was measured at 80°C for this purpose.

Immersion tests on single coupons (1 x 2 cm) were performed at 150°C. The weight gain was measured after varying exposure time to obtain uniform corrosion kinetics.

RESULTS AND DISCUSSIONS

During the initial stage of the crevice corrosion in Brine A (first few days immersion) a very thin multicolored corrosion product was observed (Fig. 1). This film was found to be the anatase form of TiO_2. For exposures of over two weeks the largest samples (2 x 4 cm) with the smallest crevice gap showed a thicker black corrosion product (Fig. 2). This was composed of the rutile form of TiO_2 with traces of lower oxides such as Ti_3O_5. Higher O_2 concentrations promote rutile formation. In general, lower pH, larger sample sizes, and smaller crevice gaps gave higher crevice corrosion rates. In order to understand the crevice corrosion mechanism, measurements of the open-circuit corrosion potentials were made at 80°C. These showed a breakdown of the passive film occurs as the pH of the brine falls below 1.0. Since a pH drop is expected to occur in the crevice, loss of passivation and crevice attack are also anticipated. These results are similar to the crevice corrosion of pure titanium in NaCl solution [10,11]. However, the crevice corrosion rates are much slower in TiCode-12. Mass transport calculations for oxygen inside the crevice showed a significant oxygen depletion in this region. The results imply that the compact and passive anatase form of TiO_2 [12] is no longer stable as the macroscopic concentration cell is developed. Consequently, the more porous rutile form of TiO_2 and lower oxides are probably formed in the crevice.

In the hydrogen embrittlement tests for SEN samples, the apparent stress intensity (K_Q) [13] values and hydrogen concentrations were determined and are given in Table III. At the 100 ppm hydrogen concentration level, the sample was very ductile (Fig. 3) with a slanted fracture surface and it had a high K_Q value. The K_Q values for 6560 and 10900 ppm of hydrogen were decreased by a factor of about 10 compared to the 100 ppm hydrogen sample. Fractographs show both alpha phase brittle fracture and alpha-beta interface cracking (Fig. 4). These features are similar to those observed in other near-alpha titanium alloys [14,15], and implies that the formation of hydride is responsible for crack initiation [16,17].

In the hydrogen uptake tests, single coupons, as well as creviced samples, were used to check the enhanced hydrogen uptake rate caused by the breakdown of the passive film inside the crevice. As shown in Table IV, the hydrogen uptake rate in the crevice sample was significantly higher than that for the single coupons. The breakdown of the passive film inside the crevice is probably responsible for the enhanced attack. Also, the reducing environment may have slowed down oxide scale growth which in turn inhibits hydrogen penetration.

C-ring tests did not show cracking for either elastically or plastically deformed samples. However, there is a possibility that dynamic tests, or the presence of radiation-induced oxidants such as ClO_3^- or H_2O_2, may

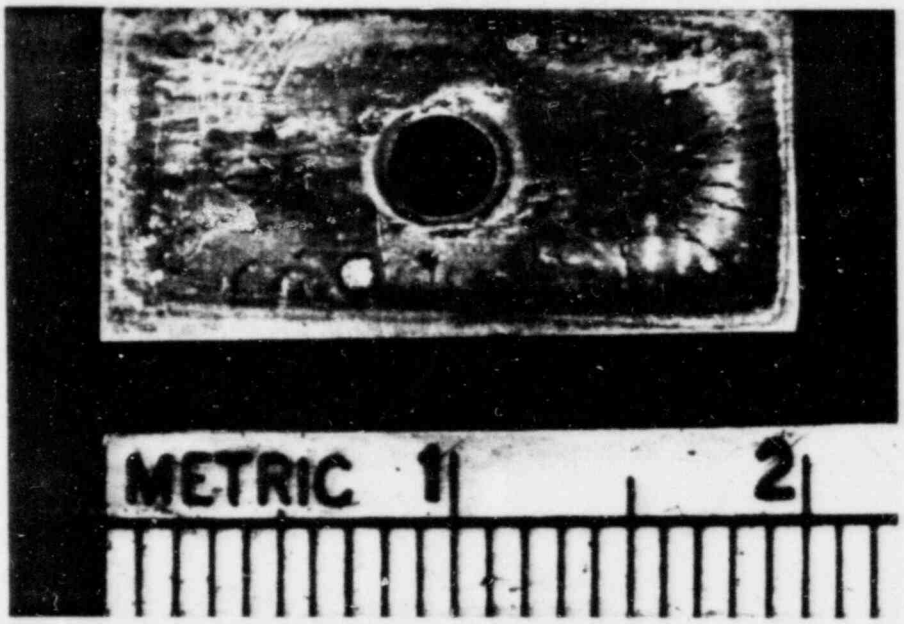

Fig. 1. The initial stage of the crevice corrosion of TiCode-12.

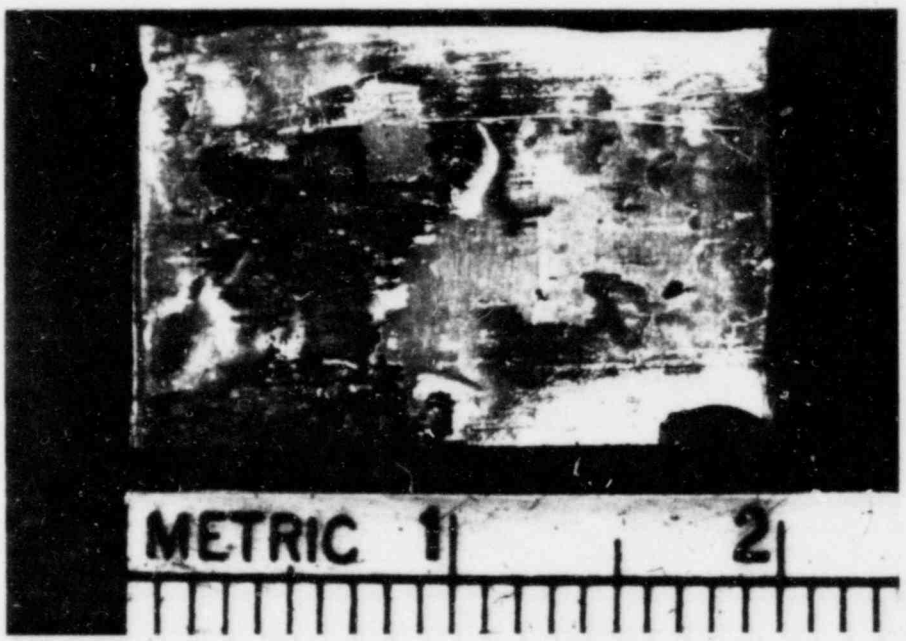

Fig. 2. Well developed crevice corrosion product on TiCode-12.

TABLE III
The apparent stress intensity factor of SEN samples at three hydrogen concentration levels

Hydrogen concentration (ppm)	100	6560	10900
Approximate K_Q (MPa$\sqrt{m}$)	43.0	6.1	5.5

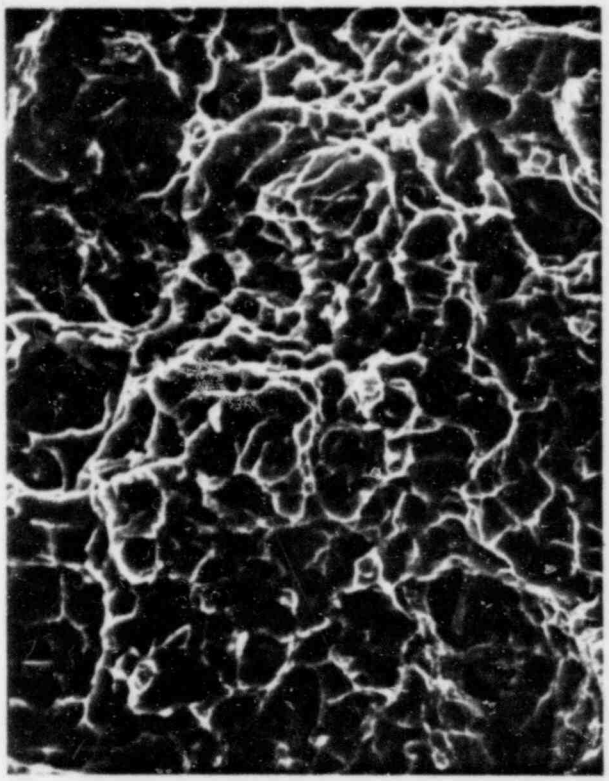

Fig. 3. Ductile fracture of TiCode-12 at 100 ppm hydrogen concentration.

Fig. 4. Brittle fracture of TiCode-12 at hydrogen concentration in access of 6560 ppm. Note the interface cracking in the center.

TABLE IV
Hydrogen uptake results (ppm) for TiCode-12 in Brine B

Run	Single coupon	Crevice samples
1	65.8	80.6 91.2
2	32.5	74.4

Note: The hydrogen concentration is 34 ppm in the as-received sample.

induce stress corrosion cracking since we observed hydrogen embrittlement and an increase in the open-circuit corrosion potential with the addition of oxidants to the brine.

Preliminary data on long term uniform corrosion rates showed that the corrosion rates decrease gradually with time. Corrosion rates are not reproducible at the present time because of the formation of precipitates (amorphous products of Mg and Si) on the samples. For the extrapolation of uniform corrosion rates to longer periods, the effect of this precipitate on the kinetics must be established.

CONCLUSIONS

The corrosion of TiCode-12 in simulated rock salt brine was investigated. The following conclusions may be drawn from this study:

- Crevice corrosion of TiCode-12 was observed at 150°C. The corrosion product was the rutile form of TiO_2 with a trace of lower oxides.
- Hydrogen caused a significant decrease in the apparent stress intensity level in fracture mechanics samples. Hydride formation is thought to be responsible for crack initiation.
- Enhanced hydrogen uptake was observed in crevice samples.
- Static C-ring tests did not show stress corrosion cracking in acidified brines.
- Extrapolating of short term uniform corrosion rate data is complicated by the presence of precipitates on the sample.

ACKNOWLEDGMENTS

Our thanks go to G. Spira and R. Jones for general technical assistance, P. Klotz and J. Forrest for their work on chemical analyses, and M. McNeil (NRC) for program coordination.

REFERENCES

1. J. W. Braithwaite, N. J. Magnani, and J. W. Munford, "Titanium Alloy Corrosion in Nuclear Waste Environments," SAND79-2023C, 1979.

2. J. W. Braithwaite and N. J. Magnani, "Nuclear Waste Canister Corrosion Studies Pertinent to Geologic Isolation," Nuclear and Chemical Waste Management, 1, 37 (1980).

3. M. A. Molecke, D. W. Schaefer, R. S. Glass, and J. A. Ruppen, "Sandia HLW Canister/Overpack Studies Applicable to a Salt Repository," SAND81-1585, 1981.

4. R. E. Westerman, "Investigation of Metallic, Ceramic, and Polymeric Materials for Engineered Barrier Applications in Nuclear Waste Packages," PNL-3484, 1980.

5. S. G. Pitman, "Investigation of Susceptibility of Titanium-Grade 2 and Titanium-Grade 12 to Environmental Cracking in a Simulated Basalt Repository Environment," PNL-3914, 1981.

6. R. Dayal et al., "Nuclear Waste Management Technical Support in the Development of Nuclear Waste Form Criteria for the NRC, Task 1: Waste Package Overview," NUREG/CR-2333, Vol. 1, BNL-NUREG-51458, 1982.

7. T. M. Ahn et al., "Nuclear Waste Management Technical Support in the Development of Nuclear Waste Form Criteria for the NRC, Task 4: Test Development Review," NUREG/CR-2333, Vol. 4, BNL-NUREG-51458, 1982.

8. G. H. Koch, A. J. Bursle, R. Liu, and E. N. Pugh, "A Comparison of Gaseous Hydrogen Embrittlement, Slow-Strain-Rate Embrittlement, and Stress Corrosion Cracking in Ti-8Al-1Mo-1V," Met. Trans. A. 12A, 1833 (1981).

9. "Standard Recommended Practice for Making and Using C-Ring Stress Corrosion Test Specimens," ASTM G38-73 Annual Book of ASTM Standards, Part 10, Metals - Physical, Mechanical, and Corrosion Testing, (ASTM, Philadelphia 1979) p. 854.

10. J. C. Griess, Jr., "Crevice Corrosion of Titanium and Aqueous Salt Solutions," Corrosion-NACE 24, 96 (1968).

11. J. D. Jackson and W. K. Boyd, "Crevice Corrosion of Titanium," Applications Related Phenomena in Titanium Alloys, ASTM STP 432, (ASTM, Philadelphia 1968) p. 218.

12. N. D. Tomashov, G. P. Chernova, Y. S. Ruscol, and G. A. Ayuyan, "The Passivation of Alloys on Titanium Bases," Electrochemica Acta 19, 159 (1974).

13. "Standard Test Method for Plane-Stain Fracture Toughness of Metallic Materials," ASTM E-399-81 Annual Book of ASTM Standards, Part 10, Metals - Physical, Mechanical, and Corrosion Testing, (ASTM, Philadelphia 1979) p. 540.

14. D. A. Meyn and G. Sandoz, "Fractography and Crystallography of Subcritical Crack Propagation in High Strength Titanium Alloys," Met. Trans. 245, 1253 (1969).

15. M. J. Blackburn and J. C. Williams, Fundamental Aspects of Stress Corrosion Cracking, R. W. Staehle, A. J. Forty, and D. VanRooyen eds. (NACE, Houston 1969) p. 620.

16. N. R. Moody and W. W. Gerberich, "Hydrogen Induced Slow Crack Growth in Ti-6Al6V-2Sn," Met. Trans. A. 11A, 973 (1981).

17. D. A. Meyn, paper presented at the TMS-AIME Fall Meeting in Niagra Falls, New York, September 1976.

NRC Research and/or Technical Assistance Rept

PAR

INTERIM REPORT BNL-NUREG-32047

Accession No._____

Contract Program or Project Title: Container Assessment

Subject of this Document: CONTAINER ASSESSMENT - CORROSION STUDY OF HLW CONTAINER MATERIALS. QUARTERLY PROGRESS REPORT, July-September 1982.

Type of Document: Interim Report

Author(s): T. M. Ahn, B. S. Lee and P. Soo.

Date of Document: October 1982.

Responsible NRC Individual and NRC Office or Division: Mr. Michael McNeil
Waste Management Branch
Division of Health, Siting and Waste Management
Office of Nuclear Regulatory Research
U. S. Nuclear Regulatory Commission
Washington, DC 20555

This document was prepared primarily for preliminary or internal use. It has not received full review and approval. Since there may be substantive changes, this document should not be considered final.

Brookhaven National Laboratory
Upton, New York 11973
Associated Universities, Inc.
for the
U.S. Department of Energy

Prepared for
U.S. Nuclear Regulatory Commission
Washington, D.C. 20555
Under Interagency Agreement DE-AC02-76CH00016
FIN A-3237